7817923

WIERCINSKI, GIORGIO MARIO
THE ACOUSTICAL DETERMINATION OF CEMENT SHEATH THICKNESS IN CASED OIL WELLS.

THE UNIVERSITY OF OKLAHOMA, DR.ENGR., 1978

University Microfilms International 300 N. ZEEB ROAD, ANN ARBOR, MI 48106

THE UNIVERSITY OF OKLAHOMA

GRADUATE COLLEGE

THE ACOUSTICAL DETERMINATION OF CEMENT SHEATH THICKNESS IN CASED OIL WELLS

A DISSERTATION

SUBMITTED TO THE GRADUATE FACULTY

in partial fulfillment of the requirements for the

degree of

DOCTOR OF ENGINEERING

BY

Giorgio Mario Wiercinski

Norman, Oklahoma

1978

THE ACOUSTICAL DETERMINATION OF CEMENT

SHEATH THICKNESS IN CASED OIL WELLS

APPROVED

DISSERTATION COMMITTEE

ABSTRACT

The Acoustical Determination ofCement
Sheath Thickness in Cased Oil Wells (April 1978)
Giorgio Mario Wiercinski, B.S., M.E., Texas A&M University
Directed by: C. R. Haden

The Cement Bond Log has normally been proposed in the current literature as a refraction analysis in which formation signals along with amplitude attenuation of casing signals are a determination of good bond between casing and formation walls.

This paper presents a different approach which also takes into account reflection analysis due to the peculiar geological configuration affecting cased well measurements in South Louisiana.

Ray theory and wave theory interact to present a solution to the travel time path required to attempt an acoustical determination of the cement thickness. The Wavefront Angle was also taken into account in the analysis since it is a major factor involved in the delay times related to the travel path.

A program was developed and implemented to be easily used in field interpretation at the well-site. The Texas Instruments programmable SR-52 with a PC-100 thermal printer, the open hole sonic log, and the CBL seismogram are all that is required to make the measurement. The ISF/SONIC provides the open hole transit time for the formation and the CBL/SEISMOGRAM provides the

cased hole factors.

Analysis of the data obtained were compared to an open-hole caliper reading. The acoustical cement determination either matched the caliper, or was in error by a maximum of 3 inches.

Snell's Law was applied and an approximation implemented by the Wavefront Angle to provide the measurement and demonstrate the reason for using reflection analysis when formation transit times are greater than cement transit time.

ACKNOWLEDGEMENTS

The author wishes to express special thanks to Dr. C. R. Haden for directing this research and providing generous assistance throughout all phases. Thanks are also due to Dr. Henry Crichlow, Dr. J. Thuren, Dr. William Cronenwett, and Dr. Ben Huey for serving as committee members at the University of Oklahoma.

Special thanks are also extended to James "Cap" Dupont, Albert Bernard, Don Cordell, Charlie Veach, Neil Mahoney, Paul Knight and "Bob" Peacock of the Western Company of North America for their discussion, advice, and technical assistance in making this field study possible.

TABLE OF CONTENTS

Chapter Page

LIST OF FIGURES

Figure		Page

LIST OF SYMBOLS

A_r	Acoustic Ray of Interest
BS	Bit Size
ID	Casing Inner Diameter
OD	Casing Outer Diameter
K	Casing Thickness
ΔT_K	Casing Transit Time
CBL	Cement Bond Log
ΔT_c	Cement Transit Time
θ	Wavefront Angle
θ_c	Cement Angle
θ_m	Mud Angle
θ_K	Casing Angle
S	Detector Spacing
DMP	Dynamic Measure Point
EFS	Effective Formation Spacing
ΔT_f	Formation Transit Time
P	Pressure
ρ	Density
k	Bulk Modulus
M	Mud Space
ΔT_m	Mud Transit Time

R	Receiver Transducer
ST	Seismogram Time
TD	Time Differential
D	Tool Diameter
T	Transmitter Transducer
W	Wavefront
ω	Radian Frequency
t	Time
V_p	Compressional Wave Velocity
V_s	Shear Wave Velocity
μ	Shear Modulus
i	Incident Angle
r	Reflected Angle
VDL	Variable Density Log
μS	Microsecond
FT	Foot

THE ACOUSTICAL DETERMINATION OF CEMENT SHEATH THICKNESS IN CASED OIL WELLS

CHAPTER I

THE CEMENT THICKNESS AND SEISMIC WAVE THEORY

Introduction

The cement thickness in a cased oil well has been a subject of interest concerning service companies involved in completion work, academicians concerned with theoretical implications, and major petroleum producers concerned with successful continuous production of oil.

One of the factors influencing the perforating qualities of casing-cement systems has been identified as the cement thickness along with other variables such as size of the explosive charge, type of gun, physical support of the casing by the cement, perforation density and other considerations as described by D. K. Smith in Chapter 12 of "Cementing Oil and Gas Wells".(1)

State Of The Art

The effects of the thickness of the cement in a borehole annulus have been studied in laboratory experiments and by observations in the field. Information on this thickness has been obtained by radiation, temperature, and acoustics as it applies to logging parameters.

Radioactive tracers injected in the cement prior to pumping the slurry in the well could be used to evaluate the sheath thickness along with a positive indication of top of cement. However, according to A. J. Teplitz[2], the principle disadvantages lie in high costs,interference with natural radioactive surveys, and health hazards.

Temperature surveys, used to indicate tops of cement by measuring the heat of hydration, have also been shown to be indicative of cement sheath thickness as described by L. W. Fowler in 1959.[3] These measurements indicate relative enlargement of boreholes by temperature gradient provided there exists a homogeneous lithology environment.

In the acoustics field the Cement Bond Log has been the principle tool diagnostic of cementing conditions. Attenuation of the casing signal and its relationship to the compressive strength of cement was investigated by Pardue et al in 1963.[4] On the basis of cement and casing variables with relation to the CBL, the casing signal attenuation provides a determination of the cement's compressive strength.

Grosmangin et al[5], in 1961, demonstrated that the attenuation of the casing signal increases with increasing cement sheath thickness. Experiments conducted on models with simulated field conditions indicated that the attenuation of the casing signal is dependent upon casing thickness, cement thickness, compressive strength of the cement, and the frequency spectrum of the acoustic pulse. When the annulus is completely filled with cured cement bonded to both casing and formation, the attenuation of the casing signal is found to be very high.

The effect of the thickness of the cement sheath on attenuation on acoustic signals was demonstrated by G. R. Pickett in 1966.[6] He concluded that if the cement sheath is thinner than 1/4 wavelength (3/4 inches), the attenuation will drop significantly.

George Suman and Richard Ellis[7] recently discussed the effects of cement sheath thickness on CBL interpretation and its related errors introduced in field operations.

Gauging borehole enlargements have been studied by J. Zemanek[8] and Chisolm & Patterson[9]. The borehole televiewer was introduced by Zemanek in 1968 and the sonar caliper by Chisolm & Patterson in 1958. Both of these tools were basically designed for open hole applications.

This dissertation examines a new technique to overcome the limitations, expense, and lack of precise results involved with the known methods describing cement thickness. The technique is based on analysis of open hole acoustic data and cased hole CBL results. Field observations taken during actual logging operations and data simulation results presented in Chapter IV and in the Appendix are used to obtain a determination of the minimum cement sheath thickness in a cased well.

The sonar caliper could be adapted to give this same information, but would require a separate logging run, therefore providing higher well operation cost. The advantage of the proposed method in this dissertation is that it utilizes existing services normally run as part of the well program, at minimum extra expense to the operator. Other methods have only been used in laboratory environments.

Decisions derived from knowing the cement sheath thickness will hopefully be a direct benefit to the well production as it involves perforating considerations of explosive charges required, minimum cement sheath damage for channeling precautions, detection of cement thief zones and other applications discussed in the appendix.

Theory of Seismic Wave Propagation

The wave equation is the basis for propagation of a disturbance in an elastic medium. There are four physical equations which are the basic relationships to derive the wave equation. They consist of Continuity, State, Motion, and Force. Their combination yields the wave equation for a perfect non-viscous fluid.[10]

The Continuity Equation:

$$\partial S/\partial t = -(\partial Vx/\partial x + \partial Vy/\partial y + \partial Vz/\partial z) \qquad \text{(I-1)}$$

Where:

$S = (p - p_o)/p_o$ is the condensation.

V is the partial velocity.

The State Equation:

$$P_o = f(\rho, T) \qquad \text{(I-2)}$$

Where:

P_o is the pressure.

ρ is the density.

T is the temperature.

For adiabatic changes, the instantaneous pressure is

$$IP = P - P_o = kS \qquad \text{(I-3)}$$

Where:

k is the bulk modulus.

The Motion Equations: (I-4)

$$fx = \rho_o aVx/ax$$

$$fy = \rho_o aVY/ay$$

$$fz = \rho_o aVZ/az$$

Where:

fx is the x component of force.

fy is the y component of force.

fz is the z component of force.

ρ_o is the equilibrium density.

<u>The Force Equations:</u> (I-5)

$$fx = -\partial P/\partial x$$

$$fy = -\partial P/\partial y$$

$$fz = -\partial P/\partial z$$

These are the force - pressure relationships.

<u>The Wave Equation:</u>

The wave equation relating pressure to x, y, z, and t is derived by the combination, addition, and differentiation of equations I-1 through I-5 to obtain

$$\partial^2 P/\partial t^2 = k/\rho_o \cdot (\partial^2 P/\partial x^2 + \partial^2 P/\partial y^2 + \partial^2 P/\partial z^2) \qquad \text{(I-6)}$$

Where:

$k/\rho_o = c^2$ is the velocity of propagation of the pressure disturbance.

<u>The Wave Theory Solution:</u>

Wave theory and ray theory are both used to solve the wave equation. Wave theory seeks solutions that satisfy the boundary and source conditions.

For example, in the case of a one-dimensional plane wave parallel to the plane of the x-axis where

$$\partial^2 P/\partial t^2 = c^2 \partial^2 P/\partial x^2 \qquad \text{(I-7)}$$

The solutions are of the form

$$P = (\text{SUM}_n A_n \text{Sin}\, k_n x + \text{SUM}_n B_n \text{Cos}\, k_n x)\ \text{SUM}_m e^{j\omega m(t-m)} \qquad \text{(I-8)}$$

where the terms inside the parentheses are specified by pressure conditions at the boundaries and the time dependent terms are specified by the source radiation properties. In practical situations the wave approach is considered to be quite complicated.

The Ray Theory Solution:

This approach considers the idea of wavefronts with rays normal to them. Wavefronts are surfaces of constant phase which satisfy the eikonal equation (eikon = image)

$$(\partial W/\partial x)^2 + (\partial W/\partial y)^2 + (\partial W/\partial z)^2 = n^2(x,y,z) \qquad \text{(I-9)}$$

where the index of refraction is

$$n = c_o/c(x,y,z) \qquad \text{(I-10)}$$

and the wavefronts are the surfaces $W(x,y,z)$ where W is called the eikonal.

The eikonal equation is useful because it is independent of time, it leads to Snell's Law, and to the curvature equations in terms of the refraction index n. Ray diagrams are made possible by the association of ray trajectories being perpendicular to

$$W(r) = (\omega t_o - \text{constant}\,) / k_o \qquad \text{(I-11)}$$

which describes a surface in space.(11)

Equation I-11 comes from assuming a solution to the wave equation as

$$\phi = A\, e^{j(k_o W - \omega t)} \qquad \text{(I-12)}$$

where A and W are functions of a position vector r, and k_o is a constant.

Wave theory is difficult to interpret as it has mathematical complexities which are not handy in practical applications. It does, however, provide a formal and complete solution to the acoustic propagation problems.

Ray theory is easy to visualize and boundary conditions can be readily inserted. It yields a quantitative picture of the distribution of sound. There are limitations since it cannot handle diffraction problems, it is independent of the source, and is valid only under restricted conditions.

Seismic Reflection and Refraction

Interpretation of seismic reflection and refraction utilizes ray theory and the travel times along ray paths. The limitations of ray theory are not considered serious in seismic profiling.

The transmission of seismic energy through solids includes the shear wave as well as the compressional wave propagation. These two types of waves have velocities given by[12].

$$V_p \; (\; (k + 1.33\mu)/\rho)^{(12)} \qquad \text{(I-13)}$$

and

$$V_s = (\mu/\rho)^{1/2} \qquad \text{(I-14)}$$

Where:

- V_p is the compressional wave velocity.
- V_s is the shear wave velocity.
- k is the bulk modulus.
- ρ is the density.
- μ is the shear modulus.

The Compressional Wave:

Compressional waves are a particular type of longitudinal wave whose direction of propagation is parallel to the direction of particle displacement. They are also known as P-Waves. The direction of propagation is away from the source. Gases, liquids, and solids have a tendency to oppose compression; therefore P-Waves can be propagated through them.

The Shear Wave:

Shear waves of S-Waves are a particular type of transverse wave whose direction of propagation is perpendicular to the direction of particle displacement. The direction of propagation is also away from the disturbance.

Because of their rigidity, solids oppose shearing forces, therefore allowing shear waves to propagate. Gases and liquids are not rigid and shear waves should not be supported through these media although there has been some discussion of shear wave propagation in fluids.

The Boundary Wave:

There are certain types of elastic waves which propagate only along boundaries which separate media of different elastic properties. They rapidly attenuate with distance from the boundary.

The wave velocities in any given medium decrease in the following order: P-Wave, S-Wave, Boundary Waves.

At boundaries in the medium where the speed or the acoustic impedance changes conversion of compressional to shear wave or vice versa can occur. In this discussion we shall be concerned mainly with the compressional wave.

The Derivation of Snell's Law:[11]

Consider the transmission and reflection of a plane acoustic wave at a boundary separating media of different densities and sound velocities. We have an (x, y, z) coordinate system with the x-axis parallel to the wavefront intersection lines and the z = 0 plane. Let the z = 0 plane be the separating boundary. Refer to figure I-1.

The plane wave

$$Pi = A\, e^{j(k_i \cdot r - \omega_i t)} \qquad \text{(I-15)}$$

is incident on the z = 0 plane with an angle of incidence i measured from the plane normal.

There will be a transmitted wave P_2 and a reflected wave P_r given as

$$P_2 = B\, e^{j(k_2 \cdot r - \omega_2 t)} \qquad \text{(I-16)}$$

$$P_r = C\, e^{j(k_r \cdot r - \omega_r t)} \qquad \text{(-17)}$$

where B and C may be complex due to phase shifts.

The propagation vectors are expressed as k's and k•r's are as follows

$$k_i \cdot r = (\omega_i / c_1)(y \operatorname{Sin} i + z \operatorname{Cos} i),$$

$$k_2 \cdot r = (\omega_2 / c_2)(y \operatorname{Sin} \theta + z \operatorname{Cos} \theta), \qquad \text{(I-18)}$$

$$k_r \cdot r = (\omega_r / c_1)(y \operatorname{Sin} r - z \operatorname{Cos} r).$$

The wave equation

$$\partial^2 P / \partial z^2 + \partial^2 P / \partial y^2 = (1/c^2)\, \partial^2 P / \partial t^2 \qquad \text{(I-19)}$$

has the solutions P_1 and P_2 in the regions of z greater than or equal to zero and less than or equal to zero respectively. The boundary conditions which must be satisfied are

$$P_1(y,0) = P_2(y,0) \qquad \text{(I-20)}$$

and at $z = 0$

$$(1/p_2)\, \partial P_2 / \partial z = (1/p_1)\, \partial P_1 / \partial z \qquad \text{(I-21)}$$

The above requires that the normal particle velocities in the two media must be equal at the boundary. In the upper media the wave P_1 is the addition of the reflected and incident waves,

$$P_1 = P_i + P_r \qquad \text{(I-22)}$$

At $z = 0$ the boundary conditions must apply for all y and t; therefore the exponents of P_i, P_2, and P_r must be equal. Then we have,

$$\omega_i = \omega_2 = \omega_r = \omega \qquad \text{(I-23)}$$

so there is no frequency change at the boundary, and

$$\operatorname{Sin} i / c_1 = \operatorname{Sin} \theta / c_2 = \operatorname{Sin} r / c_1 \qquad \text{(I-24)}$$

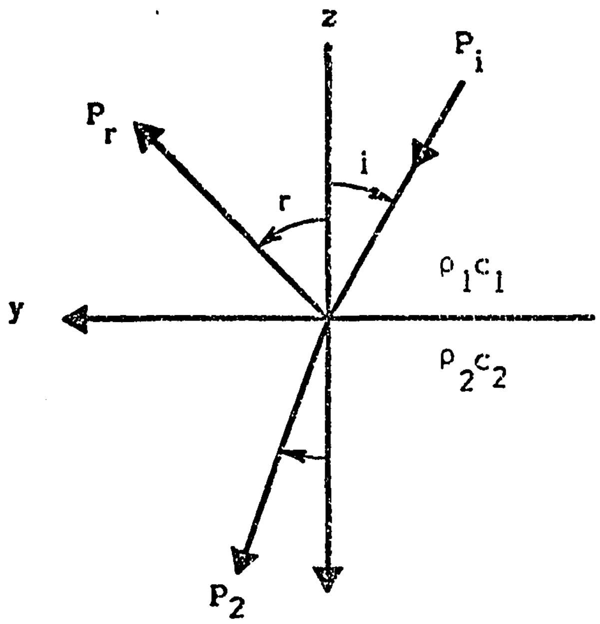

Figure I-1 Snell's Law of Reflection and Refraction

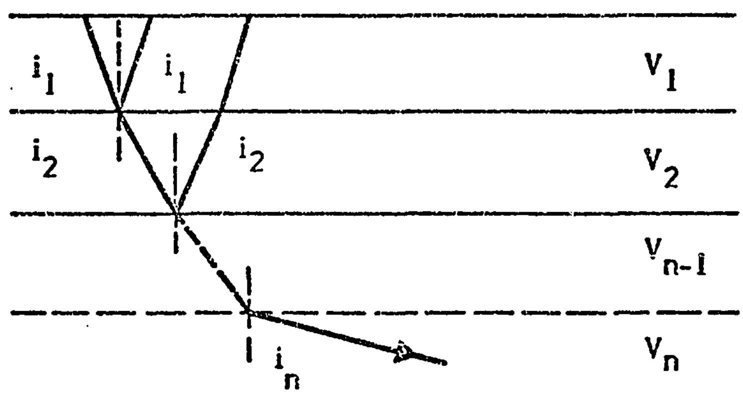

Figure I-2 Reflection and Refraction along Ray Path in Media

Equation I-24 results in Snell's Law, where the law of reflection is

Angle i = Angle r,

and the law of refraction

$$\sin i / c_1 = \sin \theta / c_2. \qquad \text{(I-25)}$$

Snell's Law:[13]

The propagation of sound along ray paths in media is governed by Snell's Law which states:

$$\sin i_1 / V_1 = \sin i_2 / V_2 = \cdots \sin i_n / V_n \qquad \text{(I-26)}$$

where V_n is the speed of the n^{th} layer.

In this manner the refraction occuring as the energy passes through different layers is described by Snell's Law as seen in Figure I-2. The Law states that for reflection at an interface, the angle of incidence is equal to the angle of reflection.

Travel Time

Reflected Waves: The Image Source Solution[13, 14]

A reflected wave traveling through a homogeneous isotropic medium of thickness h has an associated travel time given by

$$\begin{aligned} t &= (\overline{AB} + \overline{BC}) / V_1 \\ &= [(x^2 + 4h^2) / V_1^2]^{1/2} \end{aligned} \qquad \text{(I-27)}$$

obtained by the Image Source calculation as shown in Figure I-3. The equation is a hyperbola having an intercept of $2h/V_1$ at x = 0 on the t axis.

The slope of the curve is given by

$$dt/dx = x (x^2 + 4 h^2)^{-1/2} / V_1 \qquad \text{(I-28)}$$

and the ray emergence angle is obtained from

$$\begin{aligned} \sin i &= x / (x^2 + 4 h^2)^{1/2} \\ &= V_1 \, dt/dx \end{aligned} \qquad \text{(I-29)}$$

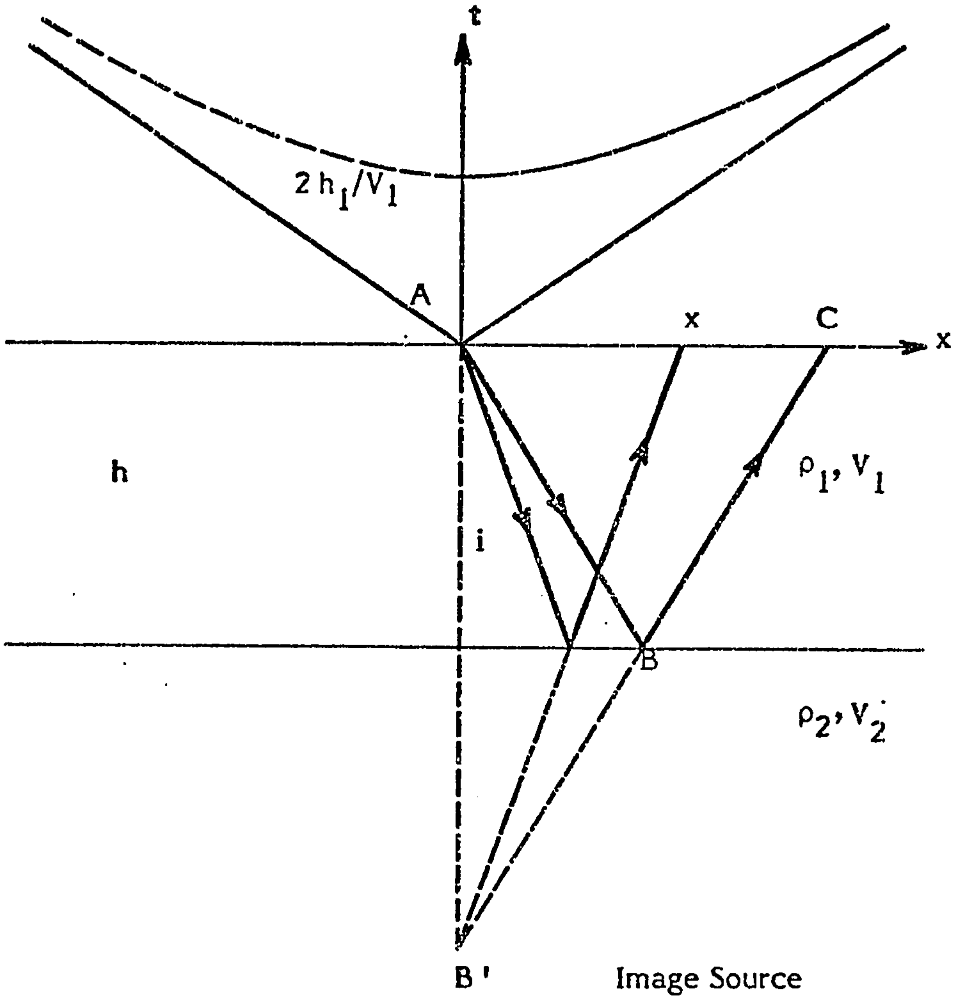

Figure I-3 The Image Source Solution in Seismic Reflection

Determination of the thickness h of the reflecting layer can be done provided the speed of propagation of a wave in that medium is known. In the case of reflection from an interface equation I-27 can be expressed as

$$t^2 = (x^2 + 4 h^2) / V_1^2 \qquad \text{(I-30)}$$

By letting $t^2 = T$ and $x^2 = X$ we then have

$$T = X / V_1^2 + 4 h^2 / V_1^2 \qquad \text{(I-31)}$$

A graph of T vs. X ($t^2 - x^2$) would be linear, the inverse slope yielding V_1^2, and the x = 0 intercept yields the layer thickness h.

Refracted Waves: The Critical Angle Solution(12)

Consider the refraction from the interface in Figure I-4 for an isotropic homogeneous layer with speed V_1 over another layer of speed V_2.

For a ray path incident on the interface and having originated in the upper media we have

$$\text{Ray Constant} = \text{Sin } i_1 / V_1 = \text{Sin } i_2 / V_2 \qquad \text{(I-32)}$$

When the angle of incidence i_1 is such that $i_2 = 90^o$

then equation I-32 becomes

$$\text{Sin } i_1 = V_1 / V_2 \qquad \text{(I-33)}$$

and the angle i is therefore

$$i = \text{Arcsin } (V_1 / V_2) \qquad \text{(I-34)}$$

The ray path in the lower media is directed along the interface and angle i_1 is called the critical angle of refraction.

Huygen's Wavefront Diagram: (13)

The Huygen wavefront diagram shown in Figure I-5 is needed to visualize how a secondary wavefront predicts the transmission of energy back to the first media. Ray theory fails to predict this energy return back to the previous media along ray paths emerging at a critical angle.

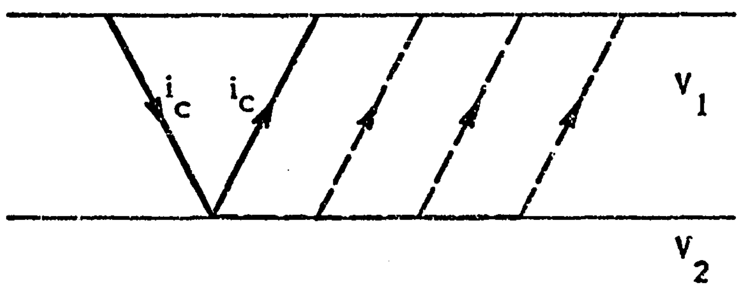

Figure I-4 Refraction from a Single Horizontal Layer with V_2 greater than V_1

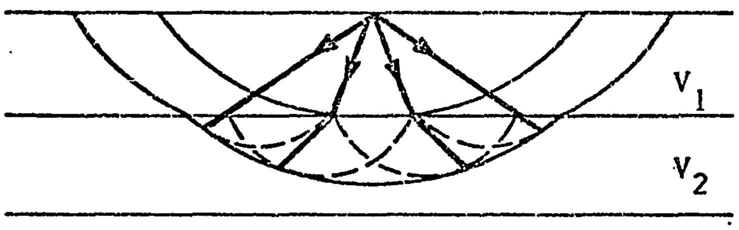

Figure I-5a Huygen Diagram wavefront in medium V_2 with V_2 greater than V_1

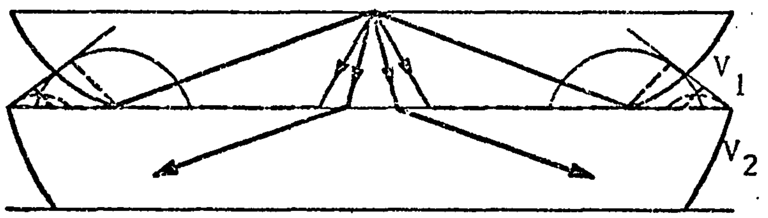

Figure I-5b Huygen's Diagram wavefront in medium V_2 and secondary wavefront emerging in medium V_1 with V_2 greater than V_1

This limitation comes from the fact that since the angle of emergence has to be obtained from

$$\theta_e = \text{Arcsin}\,(V_2 / V_1) \qquad \text{(I-35)}$$

where V_2 is greater than V_1, and a solution cannot be provided for an Arcsin greater than 1.

With Huygen's wavefront, the refracted wave in the second medium moves outward having a speed V_2 as shown in Figure I-5a. The wavefronts in the upper and lower media will be discontinuous at the boundary since V_2 is greater than V_1.

Secondary waves are emitted into the first media (see Figure I-5b) as the wave in the second media gradually moves outward, disturbing the interface. The secondary waves form a conical wavefront moving back towards the surface at the critical angle.

<u>Multi-Layer System:</u>(13, 15, 16)

The Huygen's approach can be readily applied to a multi-layer situation where V_n is greater than V_{n-1}. The travel time equations developed by C.B. Officer are given below as well as a travel time graph for the multi-layer analysis.

$$t_1 = x / V_1$$
$$t_2 = x / V_2 + (2\,h_1/V_1)\,\text{Cos}\,i_{12} \qquad \text{(I-37)}$$
$$t_3 = x / V_3 + (2\,h_1/V_1)\,\text{Cos}\,i_{13} + (2\,h_2/V_2)\,\text{Cos}\,i_{23}$$

and in general

$$t_k = x / V_k + \text{SUM}_{n=1}^{k-1}(2\,h_n/V_n)\,\text{Cos}\,i_{nk}$$

where

$$\mathrm{Sin}\ i_{nk} / V_n = 1 / V_k \tag{I-38}$$

$$n = 1, 2, \ldots\ldots, k-1$$

The multi-layer analysis is shown in Figure I-6.

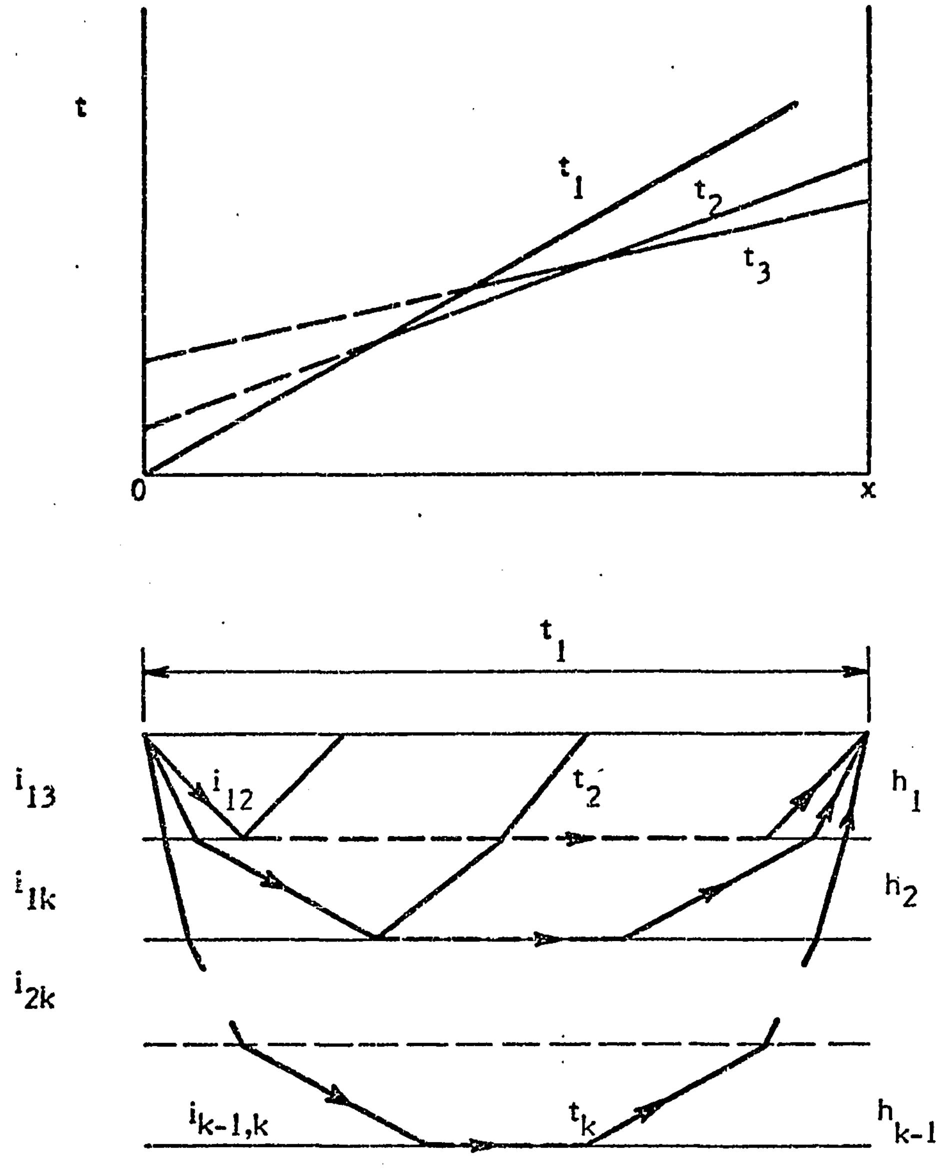

Figure I-6 Refraction and Travel Time Analysis for a Multi-Layer System with V_n greater than V_{n-1}

CHAPTER II

THE CEMENT THICKNESS DETERMINATION

THEORY

The previously developed equations for seismic reflection and refraction are applied to the ray path analysis fo a multi-layer system in a cased oil well. Snell's Law is the main pivot which permits the wavefront analysis to be simplified and allows a measurement to be made based on travel times associated with the cased environment.

Thickness determinations have been applied by the seismologists and geophysicists to determine thicknesses of horizontal layers by refraction and reflection of low frequency waves.

In this study, the same seismic principles are applied on a smaller scale in a vertical multi-layer system to determine an unknown factor - the cement thickness in the annulus between the casing and the formation wall.

Other useful information obtained from this determination is the wavefront angle associated with the measurement and the inspection technique developed to prove cement bond logs.

For this type of operation, higher frequencies are used than in seismic prospecting since the media under investigation are confined to the vicinity of the bore hole.

The Cement Bond Log:

Once the primary cementing of a well has been completed, it is necessary to verify the quality of the cement bond between the casing and the formation. This is performed to insure the isolation of different zones.

In this manner costly production losses are avoided as well as reconditioning or unnecessary secondary cement jobs.

The Cement Bond Log (CBL) is based on the amplitude attenuation of the first arrival of an acoustic signal caused by the energy transfer from the pipe and cement to the formation. The wave train (Seismogram) is the summation of all the waves arriving at the receiver from different paths.

The attenuation of the casing signal is considered to be the indication of a bonding condition between the casing and the formation. The attenuation factor for extensional waves in steel is a small fraction of one decibel per foot. There is also attenuation due to energy transfer into adjacent media which follows an exponential law (Grosmangin et al, 1961).

Experiments conducted by Grosmangin[5] indicate that the energy transfer factor is approximately one decibel per foot for free casing. Further models simulating logging conditions showed that for a bonding condition with cured cement at least one inch thick, the energy transfer factor was approximately ten times greater than for unbonded casing, ie 10 db/ft. This relative attenuation measurement provides the amplitude reduction criteria for one of the cement bond log considerations.

The casing signal is caused by the casing ray of interest comprising the mud path, casing segment traversed by the extensional wave in steel and the return mud path.

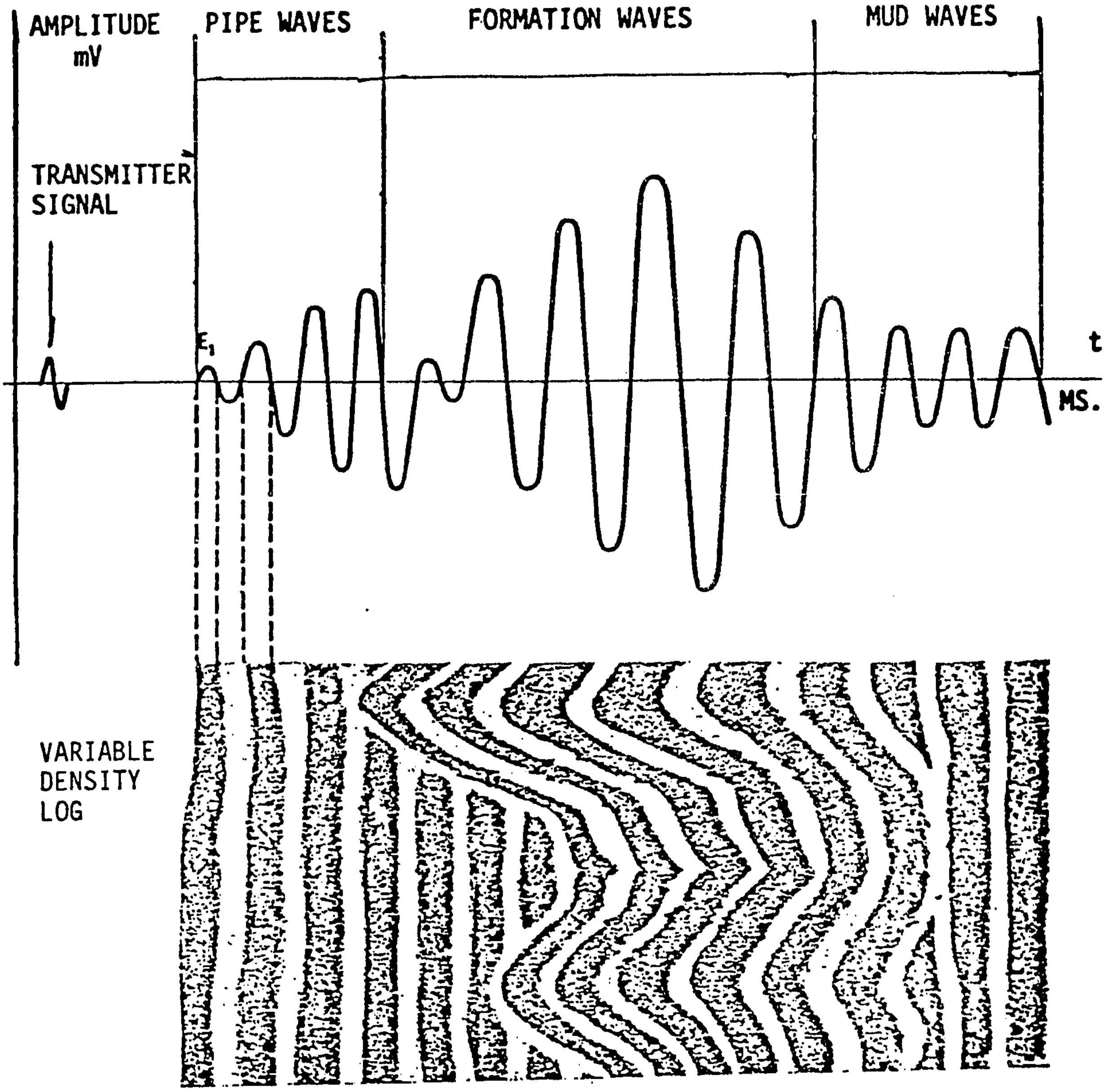

Figure II-1 General Wave Arrival Train for a Bonded Condition having Formation Returns

Courtesy of Schlumberger Inc.

Another form of presentation is known as the Variable Density Log (VDL) where black and dark grey areas represent high positive voltages, white and light grey are high negative voltages, and grey areas being intermediate. Refer to Figure II-1.

Laboratory tests have determined that the attenuation of acoustic waves in bonded pipe is directly proportional to the percentage of the circumference around the pipe having a good bond.

The typical bond tool consists of a transmitter transducer, a receiver transducer, electronic section, and a T - R spacer bar of either 3, 4, or 5 ft. The tool is normally centralized to avoid transmission loss and distortion in the receiver signal. The transmitter signal is normally filtered out of the wave train display.

The Open Hole Sonic Log:

This service is run as a formation evaluation survey which directly yields the interval transit time in microseconds per foot. This is done in the open hole with a fluid and formation interface. The open hole measurement provides the transit time for the ray path analysis used to obtain the cement thickness.

Porosity and reservoir evaluation are also obtained from the open hole sonic log.

The sonic tool presently used consists of two transmitters and four receivers geometrically arranged to compensate for bore hole effects and provide a true reading of interval transit time.

The Open Hole Caliper:

An open hole caliper is run in combination with some tools to provide a measurement of the bore hole diameter. It normally has a maximum range of 16 inches of diameter.

In the test results of Chapter III the cement thickness is compared to the effective caliper. This is a term used in this paper to describe the caliper reading after casing has been landed. It provides the space between the casing and the bore hole wall as follows

$$\text{Eff. Caliper} = (\text{Caliper} - \text{Casing O.D.})/2 \qquad \text{(II-1)}$$

An assumption has been made that the casing has been landed with centralizers and is roughly centered in the bore hole.

<u>Interpretation:</u>

The combination of the open hole data and the cased hole data permit the cement thickness measurement to be made in a bonded condition.

The interpretation consists of the analysis of the complete wave train, the amplitude attenuation of the first arrival to determine bonding, the open hole log to determine formation transit time, and picking the correct bond path arrival on the wave train.

Figure II-2 demonstrates different wave train (signature) conditions caused by diverse bonding situations.

The interpretation charts in the appendix were developed to aid in the interpretation of the signature by simulating data on the programmable calculator for different arrivals. Knowledge of the transit times involved will give the interpreter a good idea of the arrival times for each wave component.[17]

For example, with a bond tool having a 5 ft. spacer and the transit times known for:

$$\begin{aligned} \text{Casing} &= 57\ \mu\text{S./FT.} \\ \text{Mud} &= 166\ \mu\text{S./FT.} \qquad \text{(II-2)} \\ \text{Cement} &= 83\ \mu\text{S./FT.} \end{aligned}$$

CEMENT BOND LOG - SIGNATURE

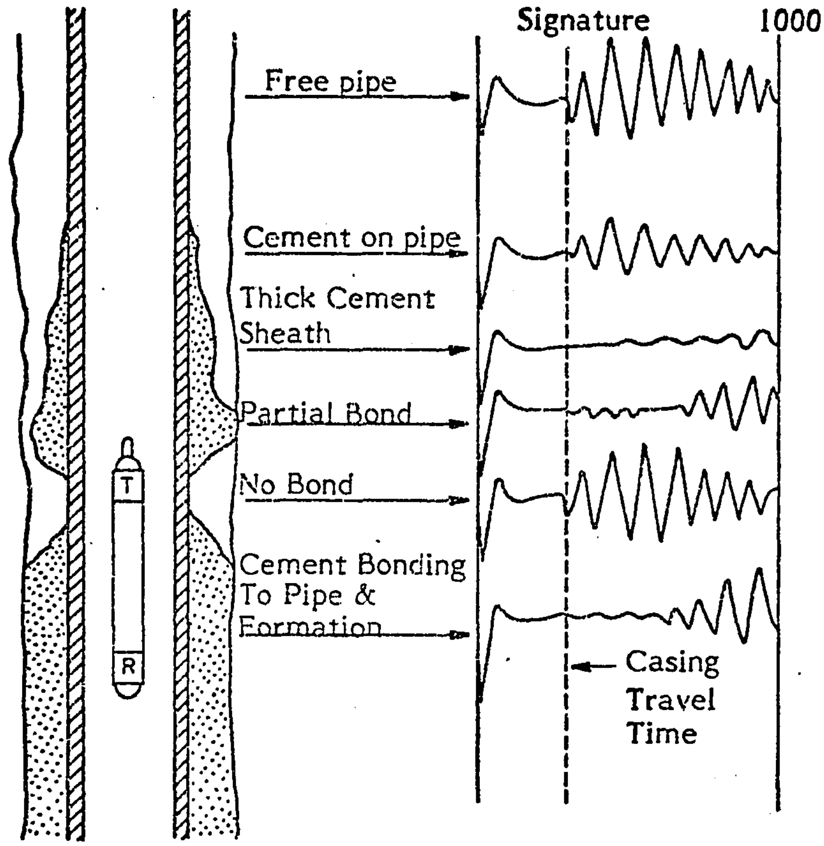

Figure II-2 CBL Signature: Oscilloscope Picture

Courtesy of the Western Co.

and the open hole sonic gives a formation having an interval transit time of 50 μS./FT. we then have the following arrivals approximated:

$$\begin{aligned} &\text{Casing} && = 5 \times 57 = 285\ \mu S. \\ &\text{Mud} && = 5 \times 166 = 830\ \mu S. \\ &\text{Formation} && = 5 \times 50 = 250\ \mu S. \end{aligned} \qquad \text{(II-3)}$$

This would mean that the arrival of the formation signal could be ahead of casing time.

When running the interpretation on the TI-SR 52 Programmable calculator the program decides whether to choose a reflection or a refraction based on the open hole comparison.

The cement transit time is considered to be 83.3 μS./FT. for various types of cement after a minimum curing time of 48 hours to achieve sufficient compressive strength.

If the transit time of the formation is lower than that of the cement, the arrival we see on the wave train is from a reflection at the cement and formation boundary. According to Snell's Law a refraction is not allowable whenever V_1 is greater than V_2.

For practical purposes, we have to use transit times in the analysis since velocities are not common in logging operations, in so far as data formating is concerned. The interval transit time is the inverse of the velocity and is:

$$\Delta T = 1{,}000{,}000 \,/\, V \qquad \text{(II-4)}$$

which is usually expressed in Microseconds / Foot.

Snell's Law therefore is interpreted as

$$\theta = \text{Arcsin}\left(\Delta T_2 \,/\, \Delta T_1 \right) \qquad \text{(II-5)}$$

From the data simulation in the cement thickness charts, cement reflection waves are expected to interfere with the attenuated pipe waves after 420 microseconds (5 x 83.3) for a 5 Ft. spacing. Should the pipe waves be completely attenuated then the first arrival seen is that of the cement wave.

CEMENT THICKNESS EQUATIONS: REFRACTED WAVES

During an acoustic event, waves will propagate in all directions in a spherical manner. The ray that causes a wave to propagate down the borehole wall at a ninty degree angle is called the ray of interest. The angle causing the vertical displacement from the previous media is called the critical angle θ. Refer to Figure II-3.

1. According to Snell's law of acoustic refraction through different media, the critical angle in a cased well is:

$$\theta = \text{Arcsin} (\Delta T_f / \Delta T_c) \qquad \text{(II-6)}$$

Where:

ΔT_c = Cement Transit Time

ΔT_f = Formation Transit TIme

The cement transit time is a known factor and the formation transit time is previously computed by the open hole sonic log.

2. Mud Delay:

The acoustic signal is delayed by the travel time equation dependent on twice the mud space M, critical angle θ, and the mud transit time ΔTm.

$$\text{Mud Time} = (2M / \cos\theta)(\Delta T_m / 12)$$

$$= (M \Delta T_m)/(6 \cos \theta)\ \mu S. \qquad \text{(II-7)}$$

ΔT_m is divided by 12 to change the μ S./FT. unit to a common μS./IN. base unit.

3. Casing Delay:

The acoustic signal is delayed by the travel time equation dependent on twice the casing thickness K, critical angle θ, and the casing transit time ΔT_k. (II-8)

$$\text{Casing Time} = (2K / \cos\theta)(\Delta T_k / 12)$$

$$= (K \times \Delta T_k)/(6 \cos\theta)\ \mu S.$$

ΔT_k is divided by 12 for base unit purposes and K is obtained by subtracting the casing I.D. from the O.D.

$$K = O.D. - I.D.\ IN. \qquad \text{(II-9)}$$

4. Effective Formation Spacing:

The length of the formation sampled by the ray of interest is dependent on the detector spacing S, tool diameter D, Bit size BS, and critical angle θ.

$$EFS = 12S - (BS - D)\tan\theta\ IN. \qquad \text{(II-10)}$$

S is multiplied by 12 to change units from FT. to Inches.

5. Formation Delay:

The acoustic signal is delayed by the formation and is dependent on the effective formation spacing and the open hole formation transit time ΔT_f. (II-11)

$$\text{Formation Time} = (EFS)(\Delta T_f / 12)\ \mu S.$$

6. CBL Seismogram Time:

The total time that the signal is delayed in a good bonding condition is identified on the seismogram wave train as the arrival of the first compressional wave from the acoustic path of interest.

$$\text{Seismogram Time} = ST\ \mu S. \qquad \text{(II-12)}$$

7. Time Differential:

The amount of time in microseconds due to the delay caused by the mud, casing, and the formation is subtracted from the seismogram time. This operation leaves the amount of time the signal is delayed by the bonded cement.

(II-13)

$$TD = ST - \text{Mud Time} - \text{Casing Time} - \text{Formation Time}\ \mu S.$$

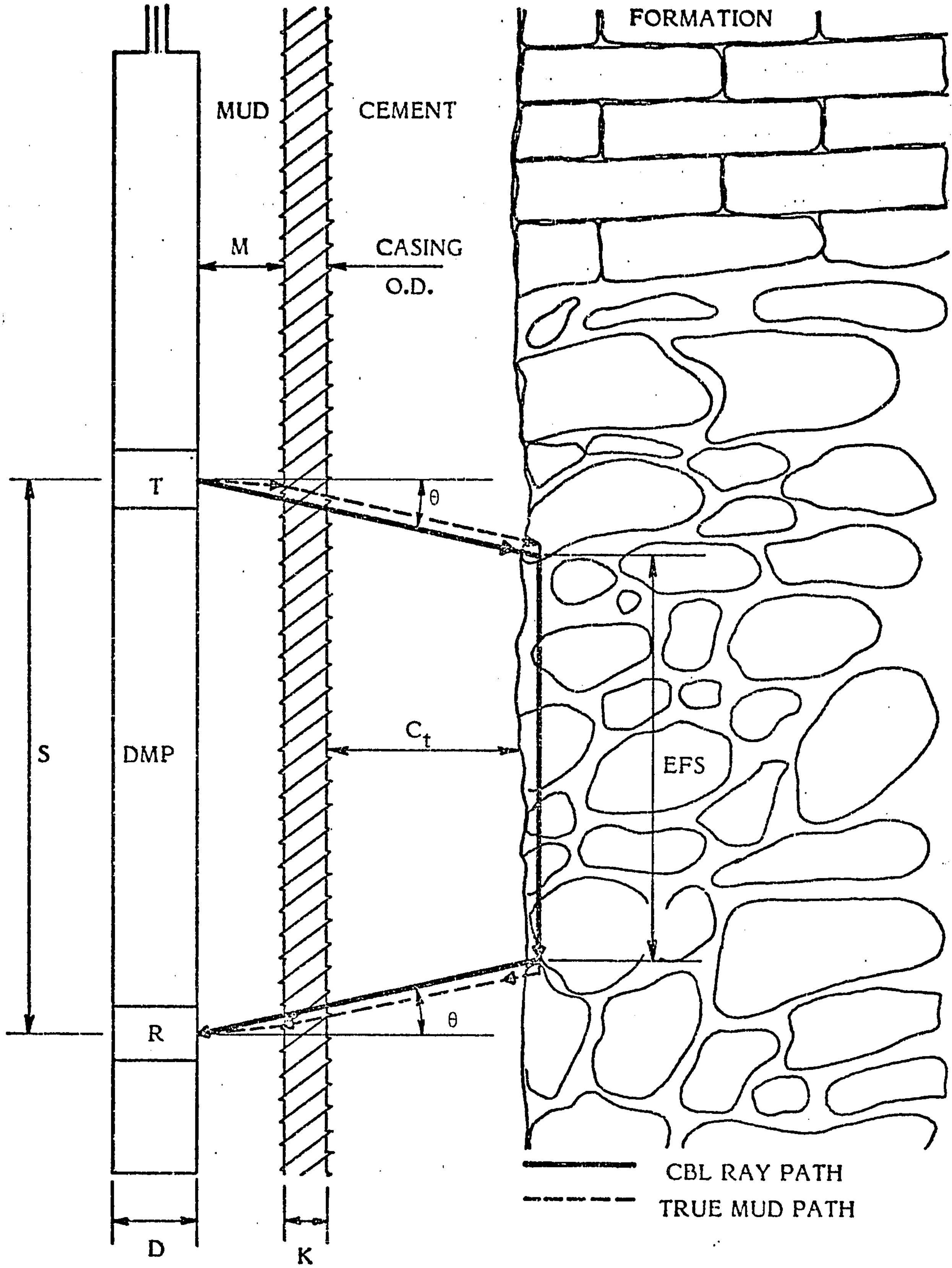

Figure II-3 Refraction Path for Formation Transit Time less than Cement transit Time

8. Cement Thickness:

The minimum amount of cement in the annulus between the casing and the formation wall is dependent on TD, critical angle θ . and transit time ΔT_c.

$$C_t = (0.5\ TD \cos\theta)/(\Delta T_c / 12)$$
$$= (6\ TD \cos\theta)/(\Delta T_c)\ \text{IN.} \qquad \text{(II-14)}$$

TD is multiplied by 0.5 to provide for half of the total travel time in cement required to make the thickness calculation.

NOTE: Cement thickness can only be determined by refraction and formation signal when ΔT_f is lower than ΔT_c. This would correspond to hard rock country. When $\Delta T_f = \Delta T_c$ it is not possible to make a calculation. In this condition the formation characteristics match those of cement.

CEMENT THICKNESS EQUATIONS: REFLECTED WAVES

When the formation transit time is greater than the cement transit time, it is not possible to obtain a refracted wave at a ninety degree angle along the cased borehole wall. Refer to Figure II-4.

In this case the first arrival of interest will be that of a reflected wave at the cement/formation interface. This may be the reason that formation time is not normally seen in a cased hole logged in South Louisiana. Most of the formation transit times in this region are greater than the transit time for cured cement.

1. According to acoustic reflection technique by the Image Source solution, the angle of reflection can be approximated as:

$$\theta = \text{Arcsin}\,(S \times \Delta T_c) / ST \qquad \text{(II-15)}$$

The cement transit time is 83.3 μS. / FT. for cured cement and the detector spacing can be either 3, 4, or 5 FT. The seismogram time ST is the first of the compressive reflected wave in the cement. A formation signal will not be seen

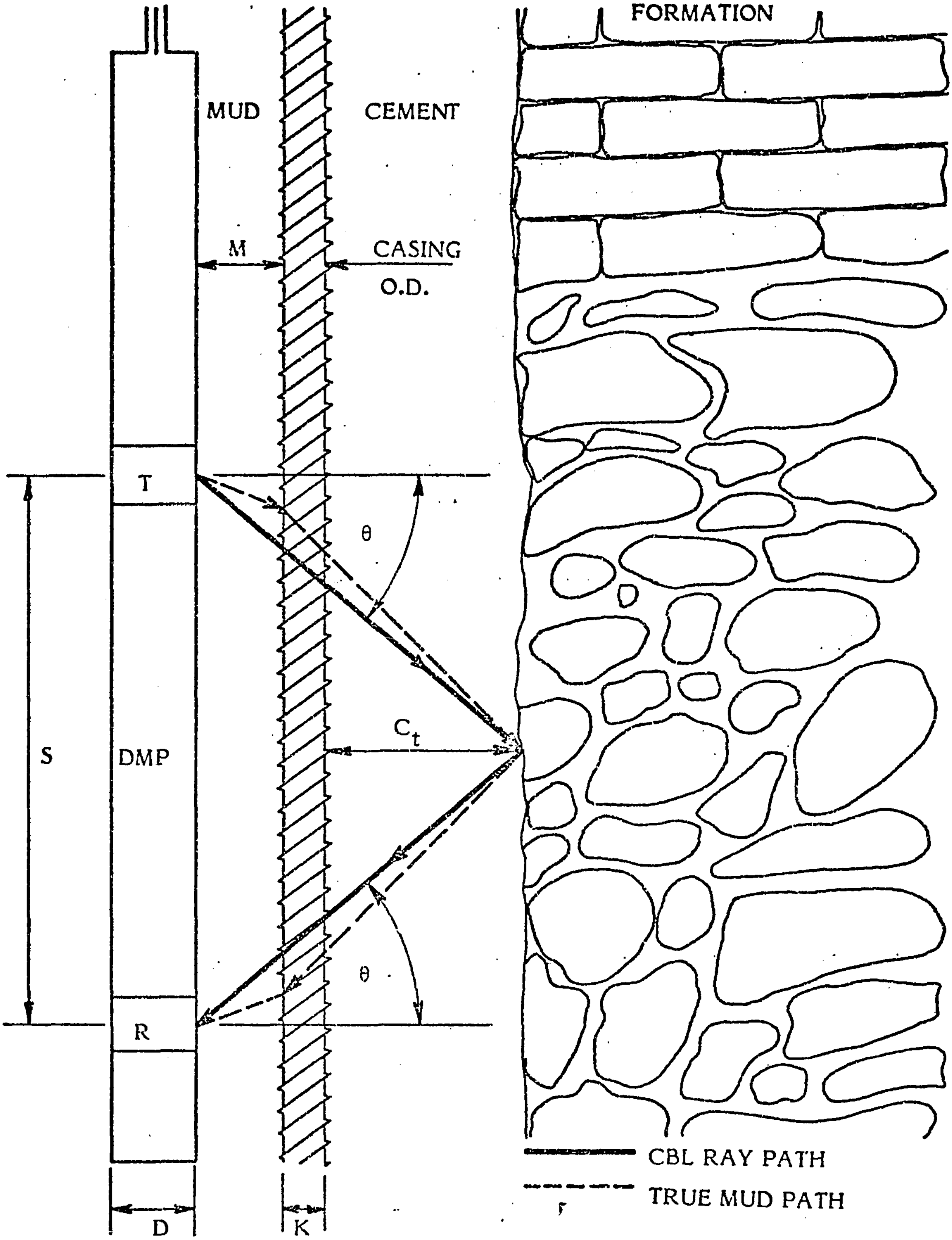

Figure II-4 Reflection Path for Formation Transit Times Greater than Cement Transit Time under these circumstances and the first arrival has a strong attenuation.

Mud Delay:

The acoustic signal is delayed by the time equation dependent on mud space M, reflection angle θ, and mud transit time T_m.

$$\text{Mud Time} = (M \ \Delta T_m)/(6 \cos\theta) \ \mu S. \qquad \text{(II-16)}$$

Mud space M is obtained by subtracting the tool diameter from the casing I.D. and dividing the result by two.

$$M = (\text{I.D.} - D)/2 \ \text{IN.} \qquad \text{(II-16)}$$

3. Casing Delay:

The signal is delayed by the time equation dependent on casing thickness K, reflection angle θ, and casing transit time ΔT_k.

$$\text{Casing Time} = (K \ \Delta T_k)/(6 \cos\theta) \ \mu S. \qquad \text{(II-17)}$$

4. CBL Seismogram Time:

The total time that the signal is delayed in a good bonding condition is identified on the wave train as the first compressional arrival ST of the cement reflected wave.

$$\text{Seismogram Time} = ST \ \mu S. \qquad \text{(II-18)}$$

5. Time Differential:

The delay caused by the mud and the casing is subtracted from ST, yielding the cement delay time.

$$TD = ST - \text{Mud Time} - \text{Casing Time} \ \mu S. \qquad \text{(II-19)}$$

6. Cement Thickness:

The minimum amount of cement in the annulus between casing and borehole wall is a function of TD, the reflection angle θ, and the cement transit

ΔT_c time

$$C_t = (6 \ TD \cos\theta)/(\Delta T_c) \ \text{IN.} \qquad \text{(II-20)}$$

NOTE: The reflection analysis must be used in formations where ΔT_f is greater than ΔT_c. This would generally correspond to soft and unconsolidated formations.

When $\Delta T_f = \Delta T_c$ it is not possible to make the cement thickness calculation since Snell's law does not allow for a reflection angle in a cased hole where the cement and formation interface theoretically does not exist. In practice, however, there is a reflected signal caused by the roughness of the borehole wall.

The Wavefront Angle Approximation:

For the mud / casing / cement / formation multi-layer system Snell's Law maintains that in the following example

MUD = 166.6 μS/FT

CASING = 57 μS/FT

CEMENT = 83.3 μS/FT

FORMATION = 70 μS/FT

$$\text{Sin } \theta_m \ \Delta T_m = \text{Sin } \theta_k \ \Delta T_k = \text{Sin } \theta_c \ \Delta T_c = \text{Sin } \theta_f \ \Delta T_f \quad \text{(II-21)}$$

The Wavefront Angle is considered to be θ_c and the rest of the ray path travel time approximated by $\theta_c = \theta_k = \theta_m$.

The justification is as follows:

The Ray Constant for a refraction at the formation interface will be 70 since $\text{Sin } \theta_f = 1$.

Since the pipe thickness is 0.5" which is less than 1/4 wavelength (10.44" for 20 KH_z) the casing is considered to be virtually transparent in a cased oil well. According to H. Guyod: "The transparency of the casing and annulus depends upon the impedance contrast for adjacent materials, the angle of incidence, the casing and annulus thicknesses and the wavelength".[12]

The mud is then where the error variation can occur. A true mud angle would be given by

$$\begin{aligned} \theta_m &= \text{Arcsin } 57/166.6 \\ &= \text{Arcsin } 0.34 \\ &= 16.6^{\circ} \end{aligned} \qquad \text{(II-22)}$$

The Wavefront Angle given by the cement / formation interface is

$$\begin{aligned} \theta_c &= \text{Arcsin } 70/83.3 \\ &= \text{Arcsin } 0.84 \\ &= 57.17^{\circ} \end{aligned} \qquad \text{(II-23)}$$

Comparing the two different mud delays for a 575 μS. seismogram time gives the following:

True Mud Delay = 46.27 μS. (II-24)

Appx. Mud Delay = 76.84 μS.

The casing delay is

The Casing Delay is

Casing Delay = 8.76 μS. (II-24)

The formation delay is

Formation Delay = 279.3 μS. (II-25)

The true time differential is found by subtracting the true mud delay + casing delay + formation delay from the Seismogram Time ST.

$$\begin{aligned} \text{True TD} &= 575 - 46.27 - 8.76 - 279.3 \\ &= 240.67\ \mu\text{S.} \end{aligned} \qquad \text{(II-26)}$$

Appx. TD = 575 - 76.84-8.76-279.3

= 210.10 µS. (II-27)

The true cement thickness and the approximate cement thickness are then compared to observe the effects of the angle variation.

True Cement Thickness = 9.39"

Appx. Cement Thickness = 8.19" (II-28)

The results of the approximation caused a 12.7% variation from the considered true value of 9.39 inches.

A true mud angle program was implemented on the Texas Instruments SR-52 calculator to compute a cement thickness measurement based on a mud/casing interface angle of incidence required to cause either a critical or a reflection angle in the cement.

<u>True Mud Angle:</u> Refraction

$$\theta_m = \text{Arcsin}[\ \text{Sin}\,\theta \times \Delta T_k \,/\, \Delta T_m\,] \qquad \text{(II-29)}$$

where θ is either a reflection or a critical angle depending on the formation encountered.

<u>True Casing Delay:</u> Refraction

$$\text{Casing Time} = (k\ \Delta T_k)/(6\ \text{Cos}\,\theta_m)\ \mu\text{sec} \qquad \text{(II-30)}$$

The results are tabulated and discussed in Chapter IV along with the results of the casing transparency wavefront angle approximation.

For the reflection analysis a new reflection angle must be calculated based on the true mud angle. Expressions for the new angles can be obtained from the following relationships:

$\text{Sin}\,\theta_m\ \Delta T_m$	$= \text{Sin}\,\theta\ \Delta T_C$	Snell's Law
S'	$= S\text{-}M\text{Tan}\,\theta_m/6$	New mud span
$\text{Sin}\,\theta$	$= S'\Delta T_C/(ST\text{-}M\,\Delta T_m \text{Cos}\,\theta_m/6)$	New reflection angle
$2\ \text{Sin}\,\theta$	$= S - 2M\text{Tan}\,\theta_m$	Tangential relationship

A matrix can be made from these relationships to obtain θ and θ_m.

$$\begin{bmatrix} 0 \\ S \\ S \end{bmatrix} = \begin{bmatrix} \Delta T_m & -\Delta T_c & 0 \\ 0 & ST/\Delta T_c & MA/6 \\ 0 & 2 & 2M \end{bmatrix} \begin{bmatrix} \text{Sin } \theta_m \\ \text{Sin } \theta \\ \text{Tan } \theta_m \end{bmatrix} \tag{II-31}$$

Where

$$A = 1 - (\Delta T_m / \Delta T_c)^2$$

Therefore we can see that for the true mud angle we have:

$$\theta_m = \text{Sin}^{-1} \left[\Delta T_c \text{Sin}\,\theta / \Delta T_m \right] \tag{II-32}$$

and for the new reflection angle we have:

$$\theta = \text{Sin}^{-1} \left[S \ \Delta T_c \,(1-A/12) / (ST - A \ \Delta T_c / 3) \right] \tag{II-33}$$

CHAPTER III

LOGGING EQUIPMENT AND TECHNIQUES

THE CBL SYSTEM

The Cement Bond Log system presents an amplitude curve to determine if there is a bond to the casing; a transit time curve which serves as a travel time indicator to determine the efficiency of the bond; the seismogram or variable intensity display for detail interpretation of the cement condition.

Instrumentation:

The instrumentation consists of a sound wave crystal transmitter to generate pulses and a transducer receiver to detect the sonic signal that has traveled through the mud, casing, cement, and the formation boundary.

The signal is transmitted to the surface via a single conductor logging cable where the signal amplitude is measured, the full wave signal is displayed on an oscilloscope, and the amplitude and transit times are recorded.

Specifications:[18]

Tool Diameter	2"
Tool Length	17.5'
Temperature Rating	350°F
Pressure Rating	20,000 PSI
TR Spacing	3,4,5, Ft.
Type Gate	Fixed Amplitude Floating Time

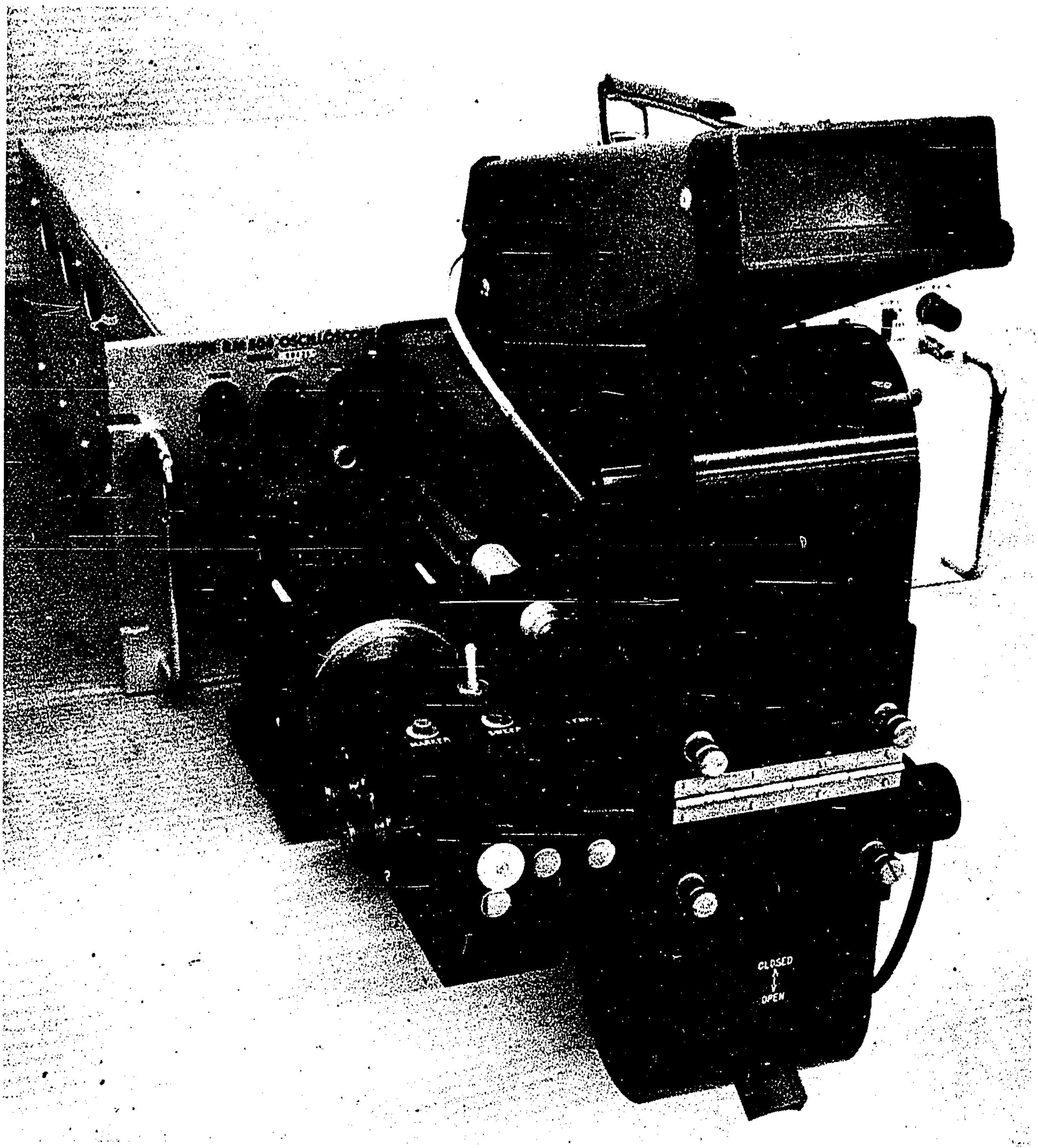

Figure III-1 70 MM Camera Mounted on RM-504 Oscilloscope for Wave Train Filming

Courtesy of The Western Co.

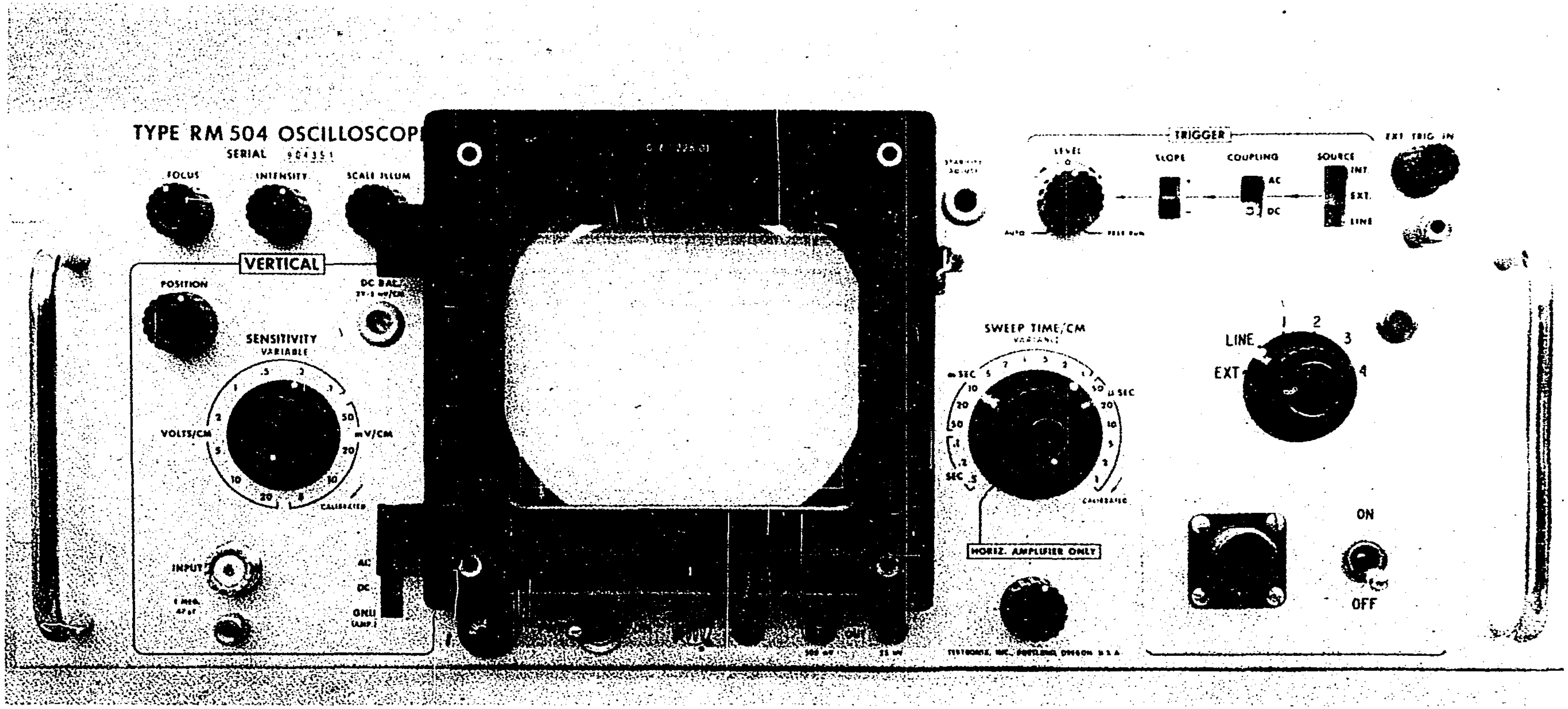

Figure III-2 RM-504 Oscilloscope Panel
Courtesy of The Western Co.

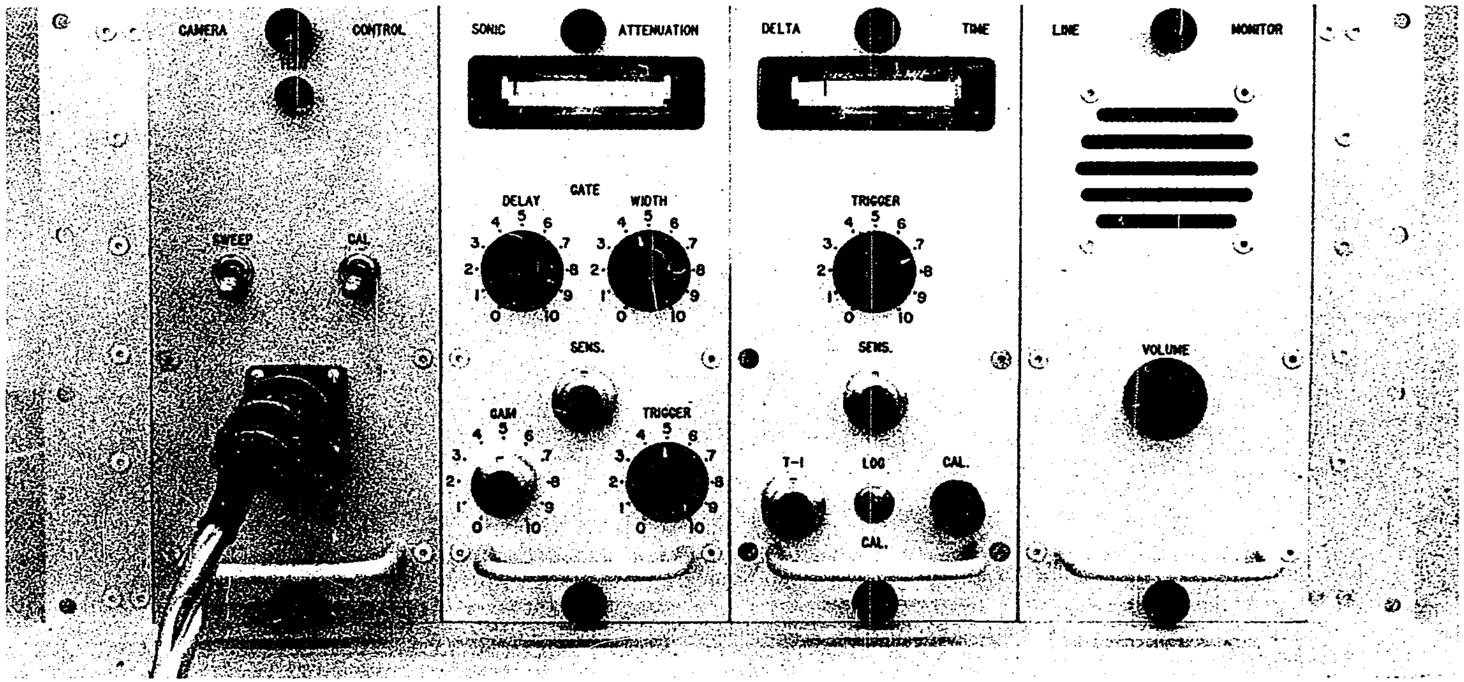

Figure III-3 CBL Surface Panels: Camera Control, Sonic Attenuation, Delta Time, Line Monitor

Courtesy of The Western Co.

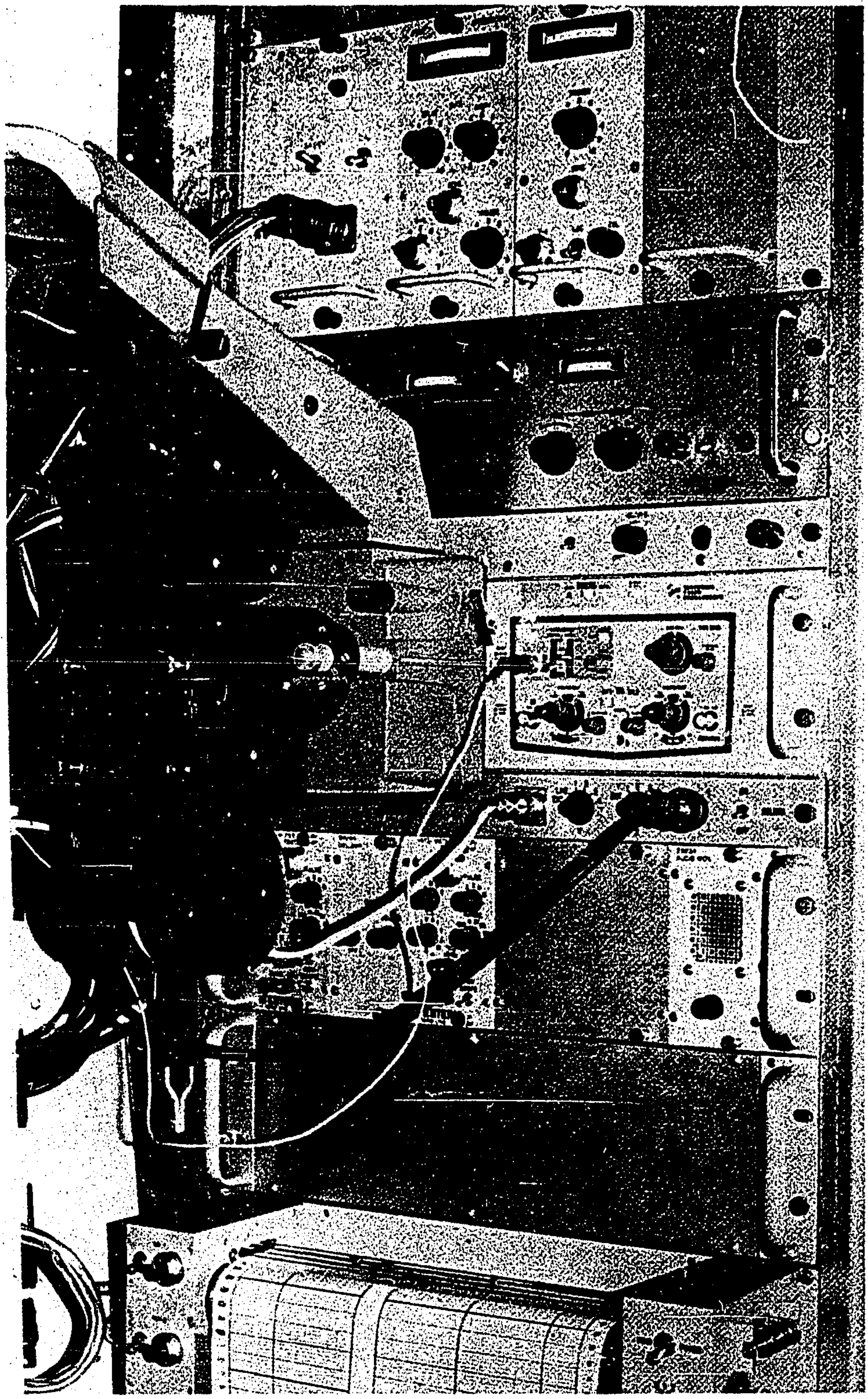

Figure III-4 CBL Surface Logging Instrumentation
Courtesy of The Western Co.

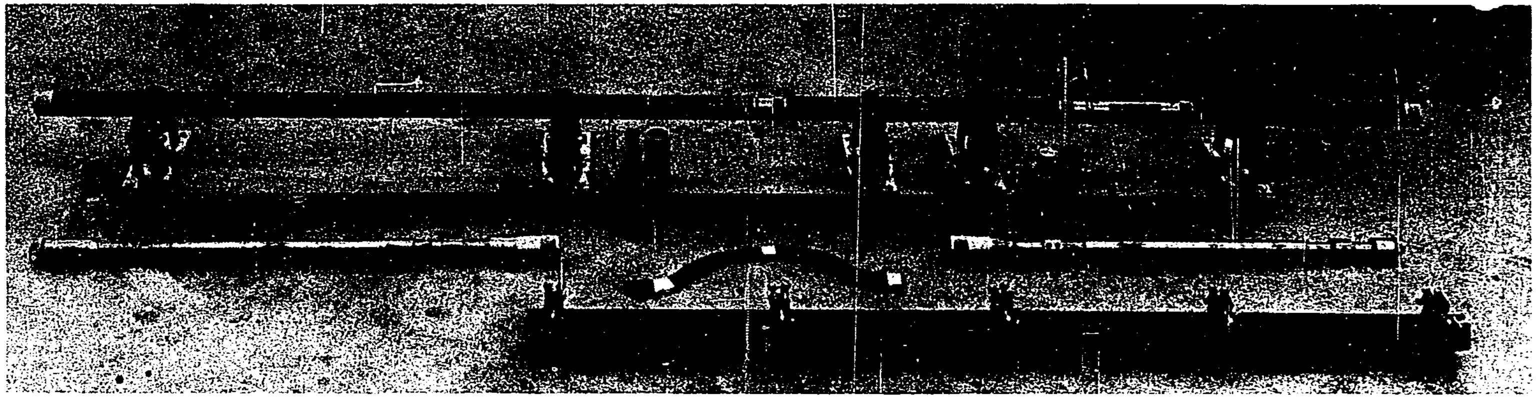

Figure III-5 2" O.D. CBL Tool and Safety Clamp

Courtesy of The Western Co.

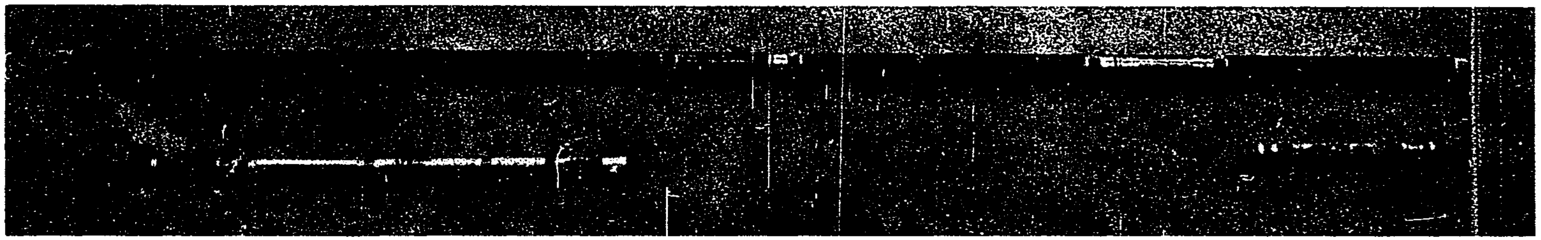

Transmitter Figure III-6 2" O.D. CBL Tool With Receiver And Transmitter Electronic Sections Receiver

Transmitter Frequency	20 KHz
Pulse Rate	20 Pulses/sec.
Gate Width (1/2 Cycle)	15-30
ΔTime Scale	200-600 μS. 200-800 μS. 200-1000 μ S. 200-1200 μ S.

THE INTERPRETATION TECHNIQUE

After the Bond Log and the Open Hole Sonic have been run the interpretation can be done at the well-site with the TI-SR 52 programmable calculator and the PC-100 thermal printer. A magnetic card with the program memory is read into the calculator memory and well conditions at the time of logging memorized in registers.

By interpreting the Bond Log the cement depths are picked and correlated to the Open Hole Log. The depth, formation transit time, and Seismogram arrival time are keyed into the SR 52 which will print out:

Depth in Feet
Wavefront Angle in Degrees
Cement Thickness in Inches

The TI-SR 52:

The Texas Instruments SR-52 can be attached to a PC-100 printer and carried in a logging unit with no difficulty. It does not take up space and can be plugged into unit power.

Operating characteristics:

Logic System	AOS
Maximum Number of Pending Operations	10
Parentheses Levels	9
Memories	20

Calculating Digits	12

<u>Programming Capability:</u>

Program Steps	224
Program Read/Write on Mag Cards	Yes
User Defined Keys	10
Possible Labels	72
Absolute Addressing	Yes
Subroutine Levels	2
Program Flags	5
Decrement & Skip on Zero (Loop)	Yes
Conditional Branching Instructions	10
Unconditional Branching	3
Indirect Branching	Yes

<u>Texas Instruments SR-52 User Instructions:</u>

LABEL A: Depth in Ft.

LABEL B: ΔT_f in μS./Ft.

LABEL C: Seismogram Time in μ S.

LABEL D: WF Angle & Cement Thickness in In.

STEP	PROCEDURE	ENTER	PRESS	DISPLAY
I	PROGRAM MEMORY			
1	Load Program	Card A	CLR 2nd Read	0
2	Load Program	Card B	2nd Read	0
II	REGISTER MEMORY			
1	Cement T.T. μS/FT	83.3	STO 0 0	83.3
2	Casing T.T. μ S/FT	57.0	STO 0 1	57.0

STEP	PROCEDURE		ENTER	PRESS	DISPLAY
3	Mud T.T.	μS/FT	166.6	STO 0 2	166.6
4	Casing OD	IN	5.5	STO 0 3	5.5
5	Casing ID	IN	5.0	STO 0 4	5.0
6	Bit Size	IN	9.87	STO 0 5	9.87
7	Detector S	FT	5.0	STO 0 6	5.0
8	Tool Diameter	IN	2.0	STO 0 7	2.0
III	LOGGING				
1	Depth	FT	12000	A	12000
2	Open Hole	μS/FT	120	B	120
3	Seismogram	μ S	475	C	475
4	Run Program/Print			D	
	WF Angle	DEG			61.26
	Cement Thick,	IN			13.11

Refer to Figure III-7 for block diagram.

<u>The Cement Thickness / Wavefront Angle Program:</u>

The following program was developed to accept all the normal field conditions regarding:

Cement Transit Times,

Casing Transit Times,

Well Fluid Transit Times,

Casing O.D.'s

Casing I.D.'s,

Bit Sizes

Detector Spacings,

and

CBL Tool Diameters.

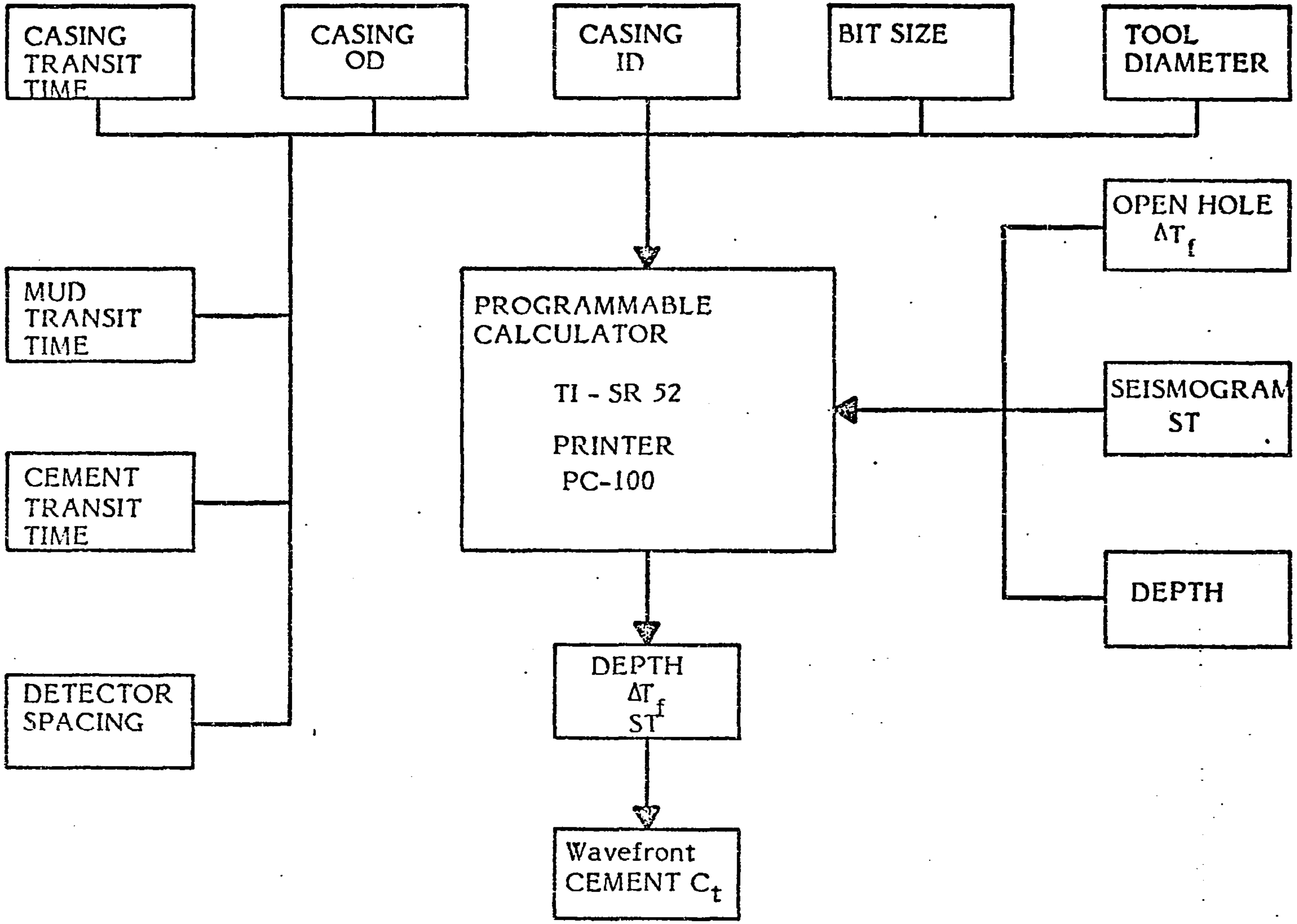

Figure III-7a Texas Instruments SR-52 Loading Scheme for Cement Thickness and Wavefront Angle Determination

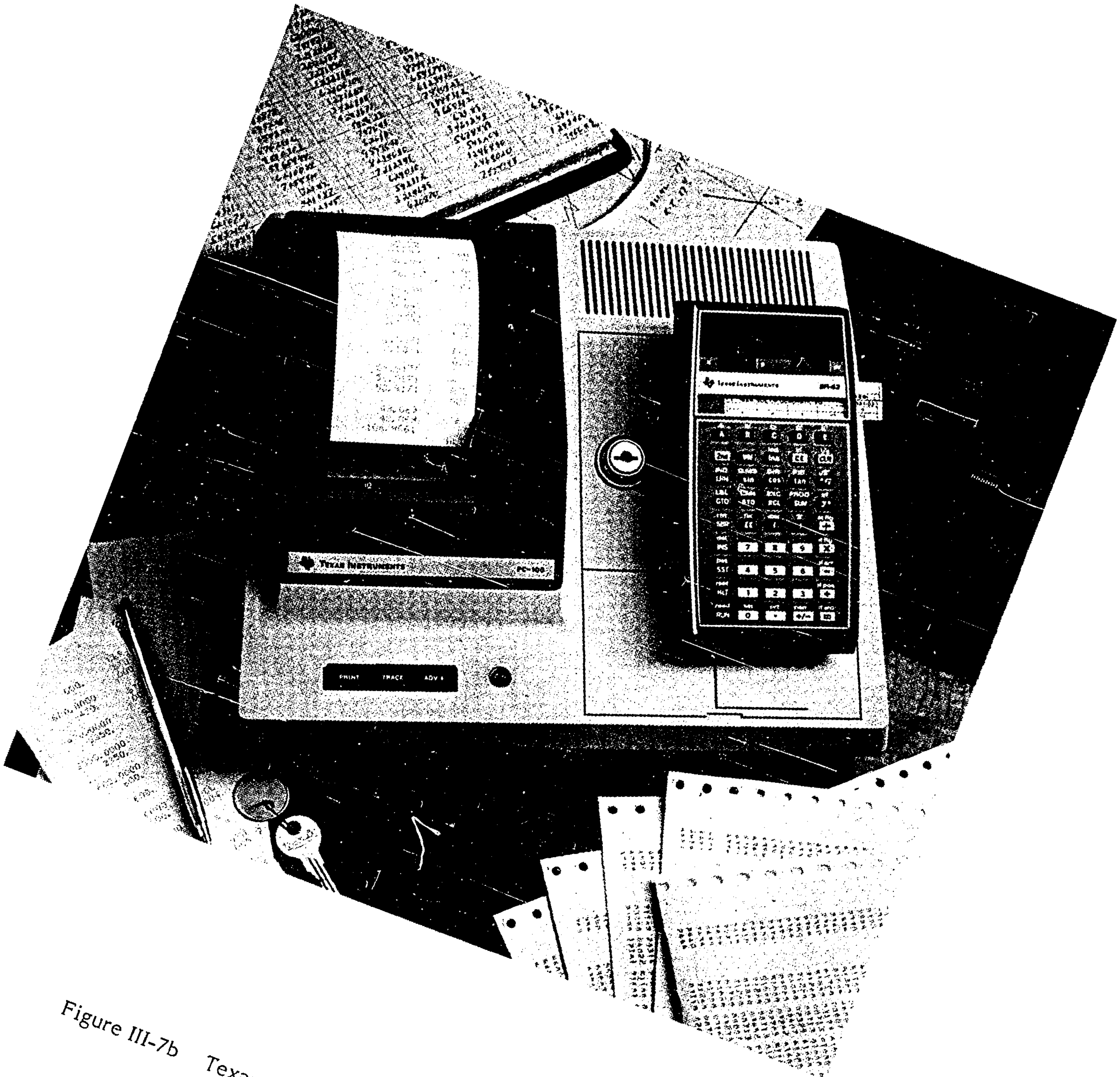

Figure III-7b Texas Instruments SR-52 with PC-100 Thermal Printer
Courtesy of Texas Instruments Inc.

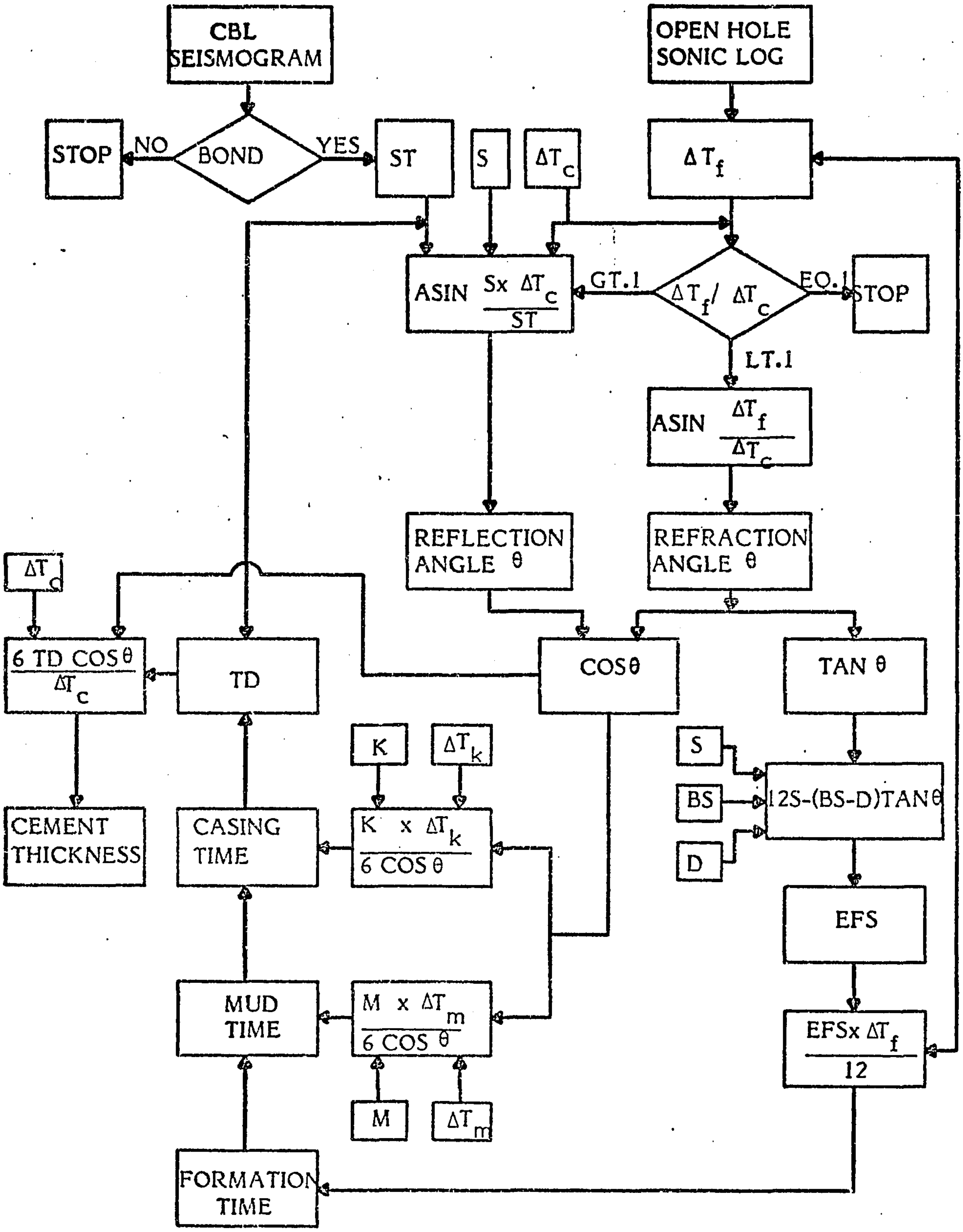

Figure III-8 Cement Thickness/Wavefront Angle Flow Chart

Any well or down-hole condition can be simulated and modeled to study the cased well environmental response.

The program is derived from the flow chart in Figure III-8 and the SR-52 language is listed in Appendix IV.

LOCATION	CODE	KEY	COMMENTS	LABELS
000	46	LBL*	Label	A Depth
001	11	A	A	B ΔT_f
002	98	prt*	Print	C ST
003	81	HLT	Halt	D Cem/WF Angle
004	46	LBL*	Label	E
005	12	B	B	A'Reflection
006	42	STO	Store	B'Subroutine
007	00	0	Register	C'Stop Test
008	08	8	08	D'
009	98	prt*	Print	E'
010	81	HLT	Halt	REGISTERS
011	46	LBL*	Label	00 ΔT_c
012	13	C	C	01 ΔT_k
013	42	STO	Store	02 ΔT_m
014	00	0	Register	03 Casing OD
015	09	9	09	04 Casing ID
016	98	prt*	Print	05 Bit Size
017	81	HLT	Halt	06 Detector S
018	46	LBL*	Label	07 Tool D
019	14	D	D	08 ΔT_f

* Press 2nd Key.

LOCATION	CODE	KEY	COMMENTS	LABELS
020	43	RCL	Recall	09 Seismogram ST
021	00	0	Register	10 $\Delta T_f / \Delta T_c$
022	08	8	08	11 θ
023	55	÷	÷	12 Cos θ
024	43	RCL	Recall	13 Tan θ
025	00	0	Register	
				REGISTERS
026	00	0	00	14
027	95	=	Equal	15
028	42	STO	Store	16
029	01	1	Register	17
030	00	0	10	18
031	75	-	-	19
032	01	1	1	FLAGS
033	95	=	Equal	0
034	90	if zero*	Test	1
035	18	C'*	Branch	2
036	80	if pos*	Test	3
037	16	A'*	Branch	4
038	43	RCL	Recall	
039	01	1	Register	
040	00	0	10	
041	22	INV	Inverse	
042	32	SIN	Sine	

* Press 2nd Key.

LOCATION	CODE	KEY	COMMENTS	REGISTERS
043	42	STO	Store	
044	01	1	Register	
045	01	1	11	
046	57	fix*	Fix	
047	02	2	Decimal 2	
048	98	prt*	Print	
049	33	COS	Cosine	
050	42	STO	Store	
051	01	1	Register	
052	02	2	12	
053	43	RCL	Recall	
054	01	1	Register	
055	01	1	11	
056	34	TAN	Tangent	
057	42	STO	Store	
058	01	1	Register	
059	03	3	13	
060	53	(	(	
061	53	(	(	
062	43	RCL	Recall	
063	00	0	Register	
064	05	5	05	
065	75	-	-	
066	43	RCL	Recall	
067	00	0	Register	

*Press 2nd Key.

LOCATION	CODE	KEY	COMMENTS	REGISTERS
068	07	7	07	
069	54	)	)	
070	65	X	X	
071	53	(	(	
072	43	RCL	Recall	
073	01	1	Register	
074	03	3	13	
075	54	)	)	
076	75	-	-	
077	53	(	(	
078	01	1		
079	02	2	12	
080	65	X	X	
081	43	RCL	Recall	
082	00	0	Register	
083	06	6	06	
084	54	)	)	
085	54	)	)	
086	65	X	X	
087	53	(	(	
088	43	RCL	Recall	
089	01	1	Register	
090	00	0	10	

* Press 2nd Key.

LOCATION	CODE	KEY	COMMENTS
091	54	)	)
092	65	X	X
093	53	(	(
094	43	RCL	Recall
095	01	1	Register
096	02	2	12
097	54	)	)
098	65	X	X
099	53	(	(
100	00	0	0.5
101	93	.	
102	05	5	
103	54	)	)
104	85	+	+
105	51	SBR	Subroutine
106	17	B'*	B'
107	46	LBL*	Label
108	16	A'*	A'
109	53	(	(
110	43	RCL	Recall
111	00	0	Register
112	06	6	06
113	65	X	X
114	43	RCL	Recall
115	00	00	Register

* Press 2nd Key.

LOCATION	CODE	KEY	COMMENTS
116	00	00	00
117	55	÷	÷
118	43	RCL	Recall
119	00	0	Register
120	09	9	09
121	54	)	)
122	22	INV	Inverse
123	32	SIN	Sine
124	42	STO	Store
125	01	1	Register
126	01	1	11
127	57	fix*	Fix
128	02	2	Decimal 2
129	98	prt*	Print
130	33	COS	Cosine
131	42	STO	Store
132	01	1	Register
133	02	2	12
134	51	SBR	Subroutine
135	17	B'*	B'
136	46	LBL*	Label
137	17	B'*	B'
138	53	(	(
139	06	6	6

* Press 2nd Key.

LOCATION	CODE	KEY	COMMENTS
140	65	X	X
141	43	RCL	Recall
142	00	0	Register
143	09	9	09
144	65	X	X
145	43	RCL	Recall
146	01	1	Register
147	02	2	12
148	75	-	-
149	53	(	(
150	53	(	(
151	43	RCL	Recall
152	00	0	Register
153	04	4	04
154	75	-	-
155	43	RCL	Recall
156	00	0	Register
157	07	7	07
158	54	)	)
159	55		
160	56	00	0
161	54	)	)
162	65	X	X

* Press 2nd Key

LOCATION	CODE	KEY	COMMENTS
163	53	(	(
164	43	RCL	Recall
165	00	0	Register
166	02	2	02
167	54	)	)
168	75	-	-
169	53	(	(
170	43	RCL	Recall
171	00	0	Register
172	03	3	03
173	75	-	-
174	43	RCL	Recall
175	00	0	Register
176	04	4	04
177	54	)	)
178	65	X	X
179	43	RCL	Recall
180	00	0	Register
181	01	1	01
182	54	)	)
183	55	÷	÷
184	43	RCL	Recall
185	00	0	Register
186	00	0	00
187	95	=	Equal

* Press 2nd Key.

LOCATION	CODE	KEY	COMMENTS
188	57	fix*	Fix
189	02	2	Decimal 2
190	98	prt*	Print
191	99	pap*	Paper Advance
192	81	HLT	Halt
193	46	LBL*	Label
194	18	C'*	C'
195	53	(	(
196	75	-	-
197	01	1	1
198	54	)	)
199	30	$\sqrt{\ }$	Square Root
200	98	prt*	Print
201	99	pap*	Paper Advance
202	81	HLT	Halt

* Press 2nd Key

CHAPTER IV

RESULTS AND CONCLUSIONS

RESULTS

Interpretations and data processing were done on three cement bond sections in two different wells. The results of the cement thickness calculation in well # A were matched against the open hole caliper and seen to be quite in agreement.

The results were graphed and the cement caliper was at the most about 2" off from the open hole caliper. In zones where the open hole reading was off scale the cement thickness measurement provided a greater than range reading.

In well # B there was no caliper run available and results were compared to the Bit Size used to drill the hole. For scientific interest, the wavefront angle was also recorded and graphed for comparison.

Simulation of the different formation transit times and seismogram arrivals were graphed and placed in the Appendix. Several tool and down-hole conditions were also modeled and graphed.

All the logs were run after the 48 hour curing time required for the cement to achieve a good compressive strength.

For well # A the logs used were the Caliper, ISF/Sonic, and CBL Seismogram. Only the ISF/Sonic and the CBL were available for well # B.

LOGGING DATA WELL # A

Well Logs:

OPEN HOLE: ISF/SONIC

CALIPER

CASED HOLE: GR/CBL SEISMOGRAM

LOGGING DATA:

1.	Cement Transit Time (48 Hrs.)	83.3 μS./FT.
2.	Casing Transit Time	57.0 μS./FT.
3.	Mud Transit Time (Lignite)	166.6 μS./FT.
4.	Casing O.D.	5 1/2 IN.
5.	Casing I.D.	5.0 IN.
6.	Bit Size	9 7/8 IN.
7.	CBL Tool Detector Spacing	5.0 FT.
8.	CBL Tool Diameter	2.0 IN.

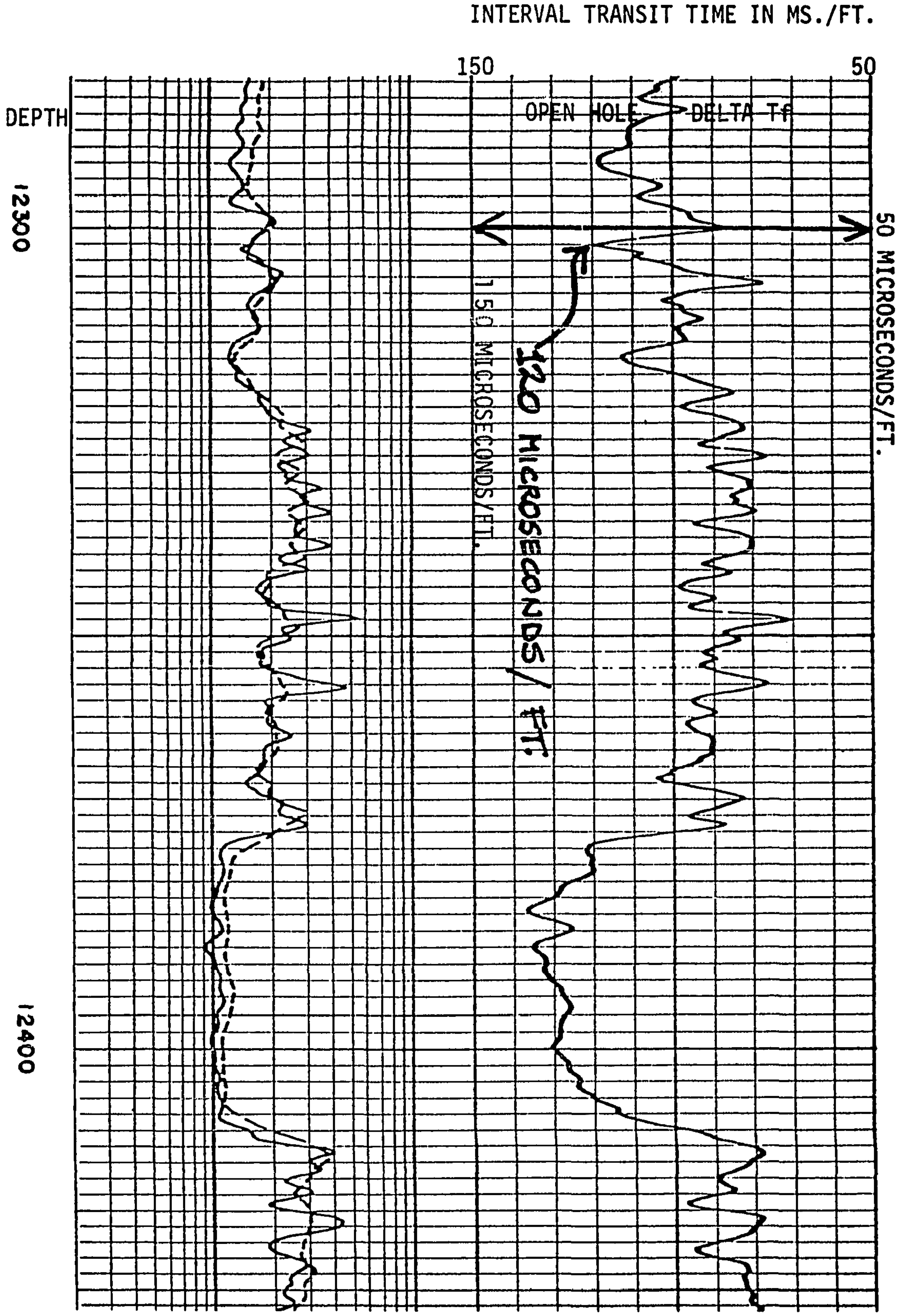

Figure IV-1 Open Hole Sonic Log of Well # A

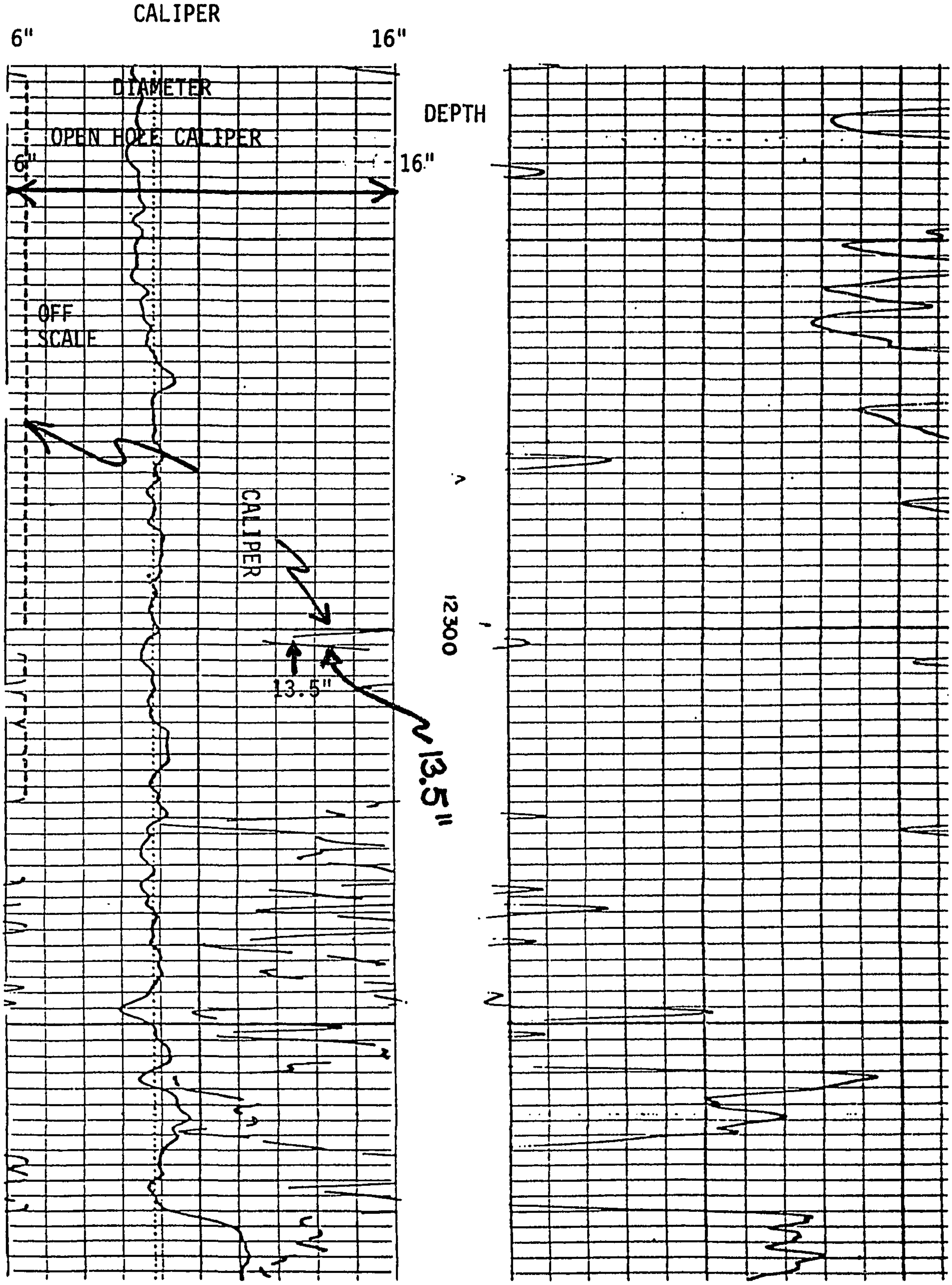

Figure IV-2 Caliper Log for Well # A

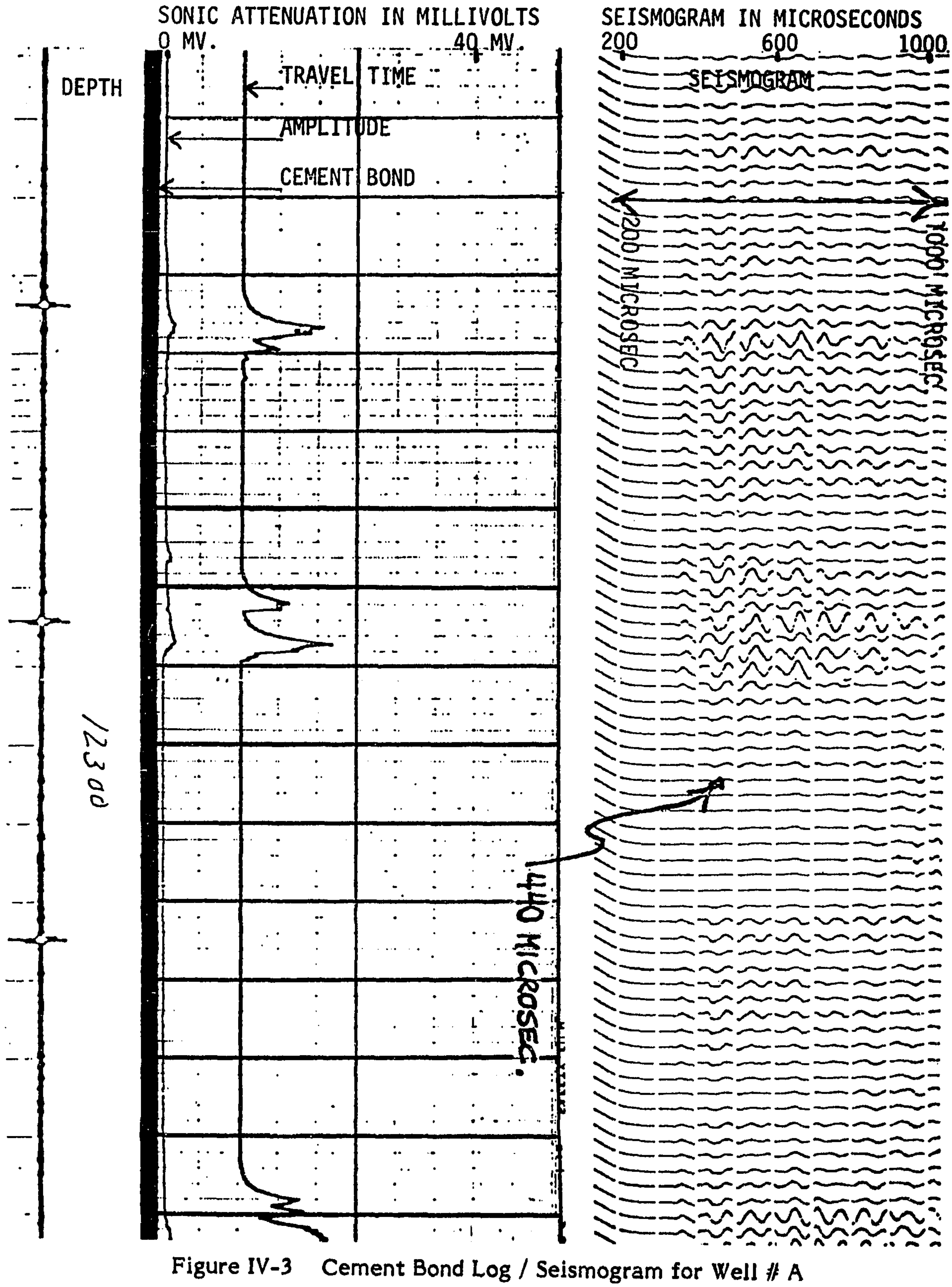

Figure IV-3 Cement Bond Log / Seismogram for Well # A

TEST RESULTS WELL # A / CALIPER

DEPTH FT.	OPEN HOLE CALIPER IN.	EFFECTIVE CALIPER IN.	OPEN HOLE SONIC DTf µS./FT.	SEISM. ST µ S.	WFA θ DEG.	CEMENT THICK IN.
12284	GT.* 16.00	GT. 5.25	108	575	46.41	25.21
12286	GT. 16.00	GT. 5.25	105	525	52.50	19.68
12288	GT. 16.00	GT. 5.25	111	525	52.50	19.68
12290	GT. 16.00	GT. 5.25	112	435	73.23	5.70
12292	GT. 16.00	GT. 5.25	118	440	71.19	6.88
12294	GT. 16.00	GT. 5.25	107	435	73.23	5.70
12296	GT. 16.00	GT. 5.25	108	435	73.23	5.70
12298	GT. 16.00	GT. 5.25	96	435	73.23	5.70
12300	16.00	5.25	87	440	71.19	6.88
12302	13.50	4.00	120	440	71.19	6.88
12304	GT. 16.00	GT. 5.25	105	450	67.75	8.93
12306	GT. 16.00	GT. 5.25	85	450	67.75	8.93
12308	15.25	4.87	96	450	67.75	8.93
12310	GT. 16.00	GT. 5.25	97	500	56.41	16.58
12312	GT. 16.00	GT. 5.25	98	490	58.21	15.25
12314	GT. 16.00	GT. 5.25	96	480	60.19	13.84
12316	GT. 16.00	GT. 5.25	112	500	56.41	16.58
12318	GT. 16.00	GT. 5.25	99	500	56.41	16.58
12320	GT. 16.00	GT. 5.25	85	440	71.19	6.88
12322	15.50	5.00	98	435	73.23	5.70
12324	14.75	4.62	82	780	79.86	5.16
12326	13.75	4.12	90	432	67.57	5.24

*GT = Greater Than

DEPTH FT.	OPEN HOLE CALIPER IN.	EFFECTIVE CALIPER IN.	OPEN HOLE SONIC DTf µS./FT.	SEISM. ST µ S.	WFA θ DEG.	CEMENT THICK IN.
12328	15.75	5.12	77	575	67.57	5.24
12330	14.30	4.40	88	430	75.60	4.36
12332	GT.* 16.00	GT. 5.25	82	800	79.86	5.41
12334	14.00	4.25	85	430	71.19	6.88
12336	12.50	3.50	95	427	77.27	3.44
12338	GT. 16.00	GT. 5.25	80	800	73.82	8.32
12340	11.20	2.85	86	425	78.52	2.75
12342	15.00	4.75	86	435	73.23	5.70
12344	13.00	3.75	98	440	71.19	6.88
12346	16.00	5.25	94	440	71.19	6.88
12348	15.80	5.15	70	575	57.18	8.22
12350	14.60	4.55	85	440	71.19	6.88
12352	12.40	3.45	92	428	76.69	3.76
12354	15.75	5.12	93	440	71/19	6.88
12356	13.30	3.90	77	510	67.57	3.46
12358	10.75	2.62	95	425	78.52	2.75
12360	12.00	3.25	94	428	76.69	3.76

*GT = Greater Than

TEST RESULTS WELL # A / CALIPER / TRUE MUD ANGLE

DEPTH FT.	MUD ANGLE DEG.	WFA θ DEG.	CEMENT THICKNESS IN.
12284	23.2	52.2	22.9
12286	25.1	58.8	17.2
12288	25.1	58.8	17.2
12290	-*	-*	-*
12292	29.8	84.1	2.5
12294	-	-	-
12296	-	-	-
12298	-	-	-
12300	29.8	84.1	2.5
12302	29.8	84.1	2.5
12304	29	77.4	5.7
12306	29	77.4	5.7
12308	29	77.4	5.7
12310	26.4	63.1	14.3
12312	27	65.2	12.7
12314	27.5	67.5	11.4
12316	26.4	63.1	14.3
12318	26.4	63.1	14.3
12320	29.8	84.1	2.5
12322	-	-	-
12324	19.5	79.8	7.3
12326	-	-	-
12328	19.5	67.5	6.9

* A calculation could not be performed due to sine function > 1.

DEPTH FT.	MUD ANGLE DEG.	WFA θ DEG.	CEMENT THICKNESS IN.
12330	-	-	-
12332	19.5	79.8	7.5
12334	-	-	-
12336	-	-	-
12338	19	73.8	10.0
12340	-	-	-
12342	-	-	-
12344	29.8	84.1	2.5
12346	29.8	84.1	2.5
12348	16.6	16.6	7.3
12350	29.8	84.1	2.5
12352	-	-	-
12354	29.8	84.1	2.5
12356	18.3	67.5	5.2
12358	-	-	-
12360	-	-	-

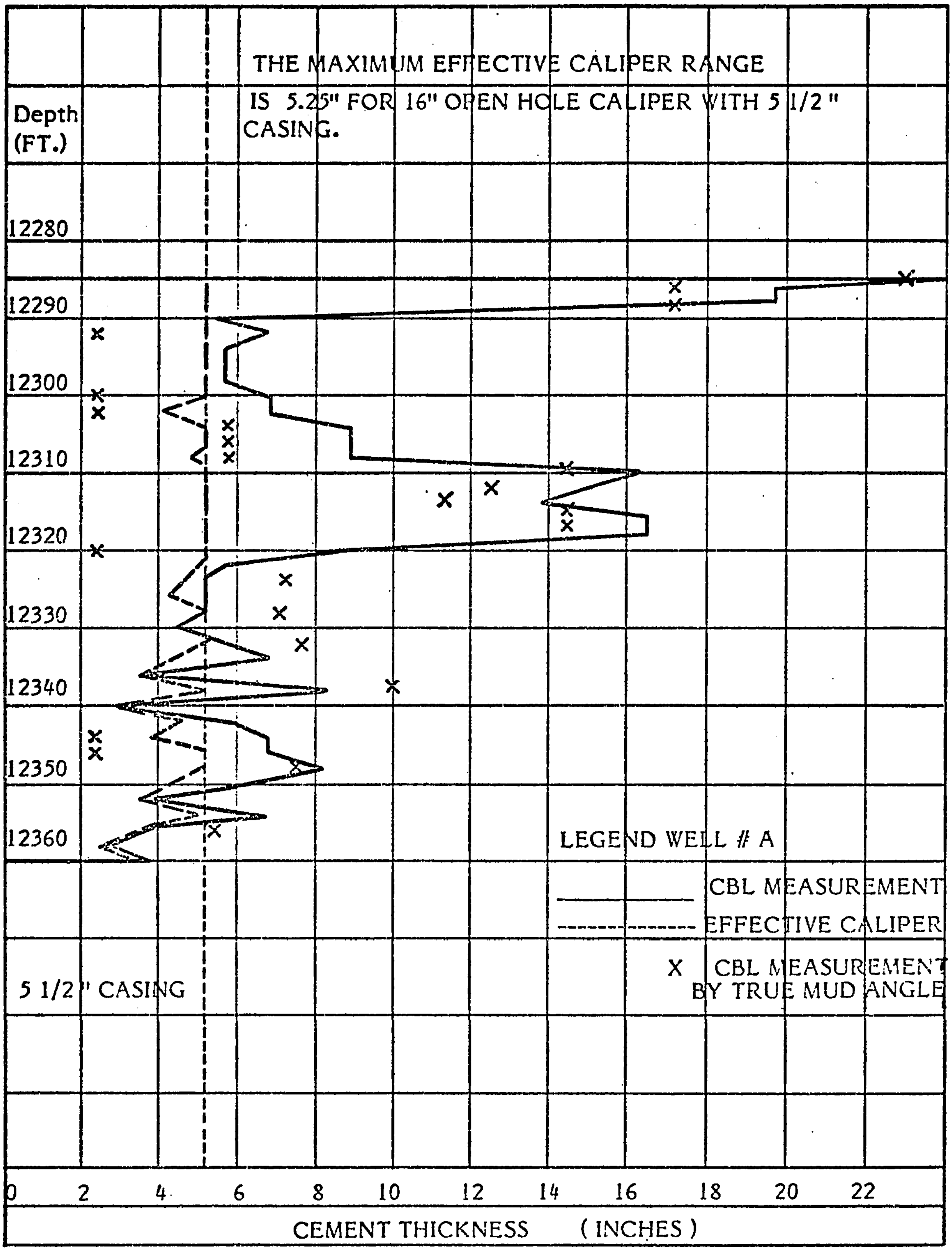

Figure IV-4 Cement Thickness vs. Open Hole Caliper for Well # A

LOGGING DATA WELL # B

WELL LOGS:

OPEN HOLE: ISF/SONIC

CASED HOLE: CBL SEISMOGRAM

LOGGING DATA:

1. Cement Transit Time (75 Hrs.)	83.3	µS./FT.
2. Casing Transit Time	57.0	µS./FT.
3. Mud Transit Time (Salt Water)	188.6	µS./FT.
4. Casing O.D.	5 1/2	IN.
5. Casing I.D.	4.70	IN.
6. Bit Size	9 7/8	IN.
7. CBL Tool Detector Spacing	5.0	FT.
8. CBL Tool Diameter	2.0	IN.

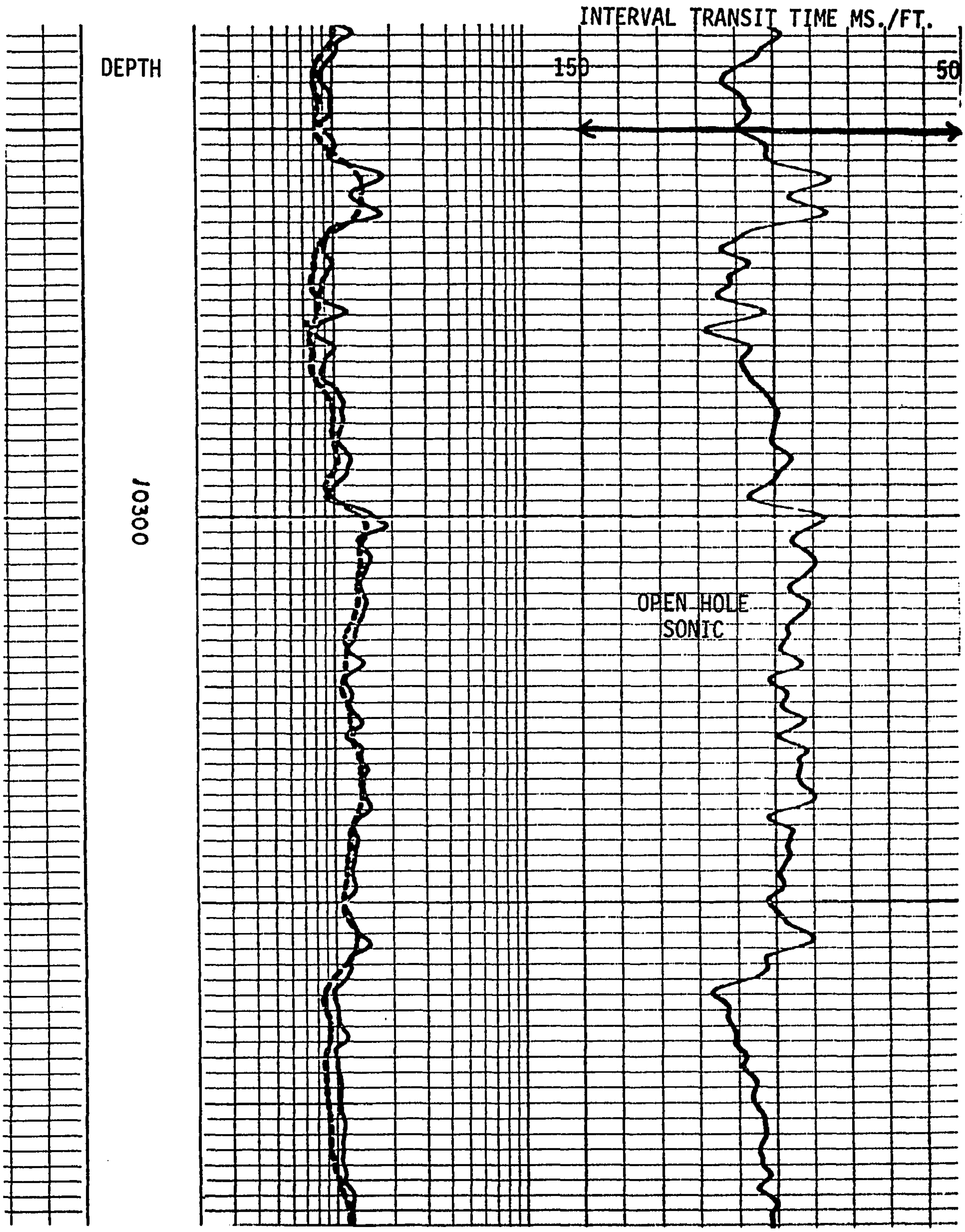

Figure IV-5 Open Hole Sonic Log for Well # B 10300 ' Zone

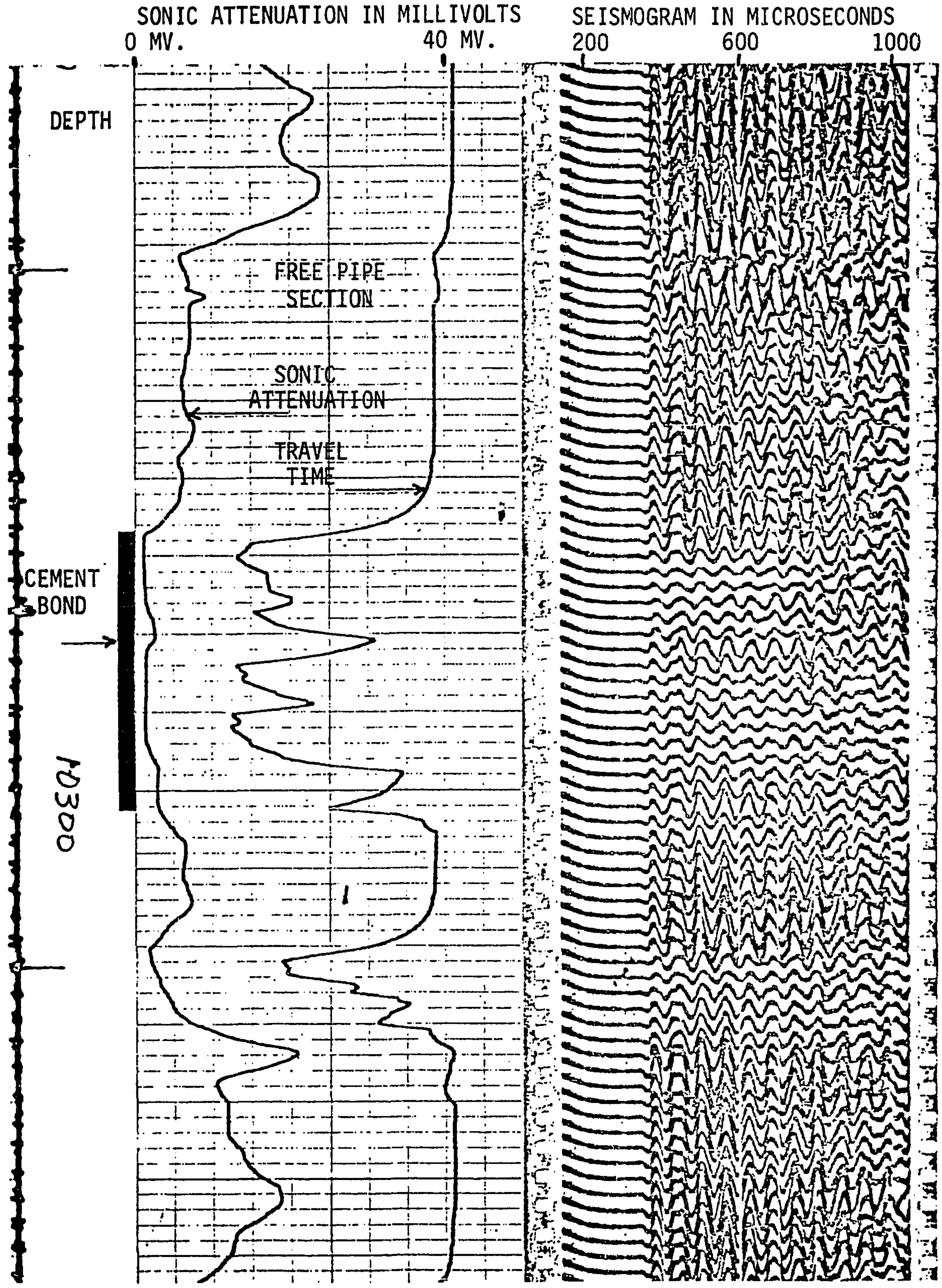

Figure IV-6 Cement Bond Log for Well # B 10300 ' Zone

TEST RESULTS WELL # B: 10300' Zone

DEPTH FT.	OPEN HOLE SONIC DTf μ S./FT.	SEISMOGRAM ST μS.	WAVEFRONT ANGLE θ DEG.	CEMENT THICKNESS IN.
10268	108	430	75.60	7.15
10270	112	430	75.60	7.15
10272	114	430	75.60	7.15
10274	103	450	67.75	11.72
10276	118	480	60.19	16.64
10278	107	445	69.38	10.74
10280	108	435	73.23	8.49
10282	106	430	75.60	7.15
10284	103	428	76.69	6.55
10286	100	450	67.75	11.72
10288	100	450	67.75	11.72
10290	101	445	69.38	10.74
10292	96	437	72.38	8.98
10294	98	425	78.52	5.54
10296	102	430	75.60	7.15
10298	106	428	76.69	6.55
10300	86	445	69.38	10.74
10302	84	435	73.23	8.49

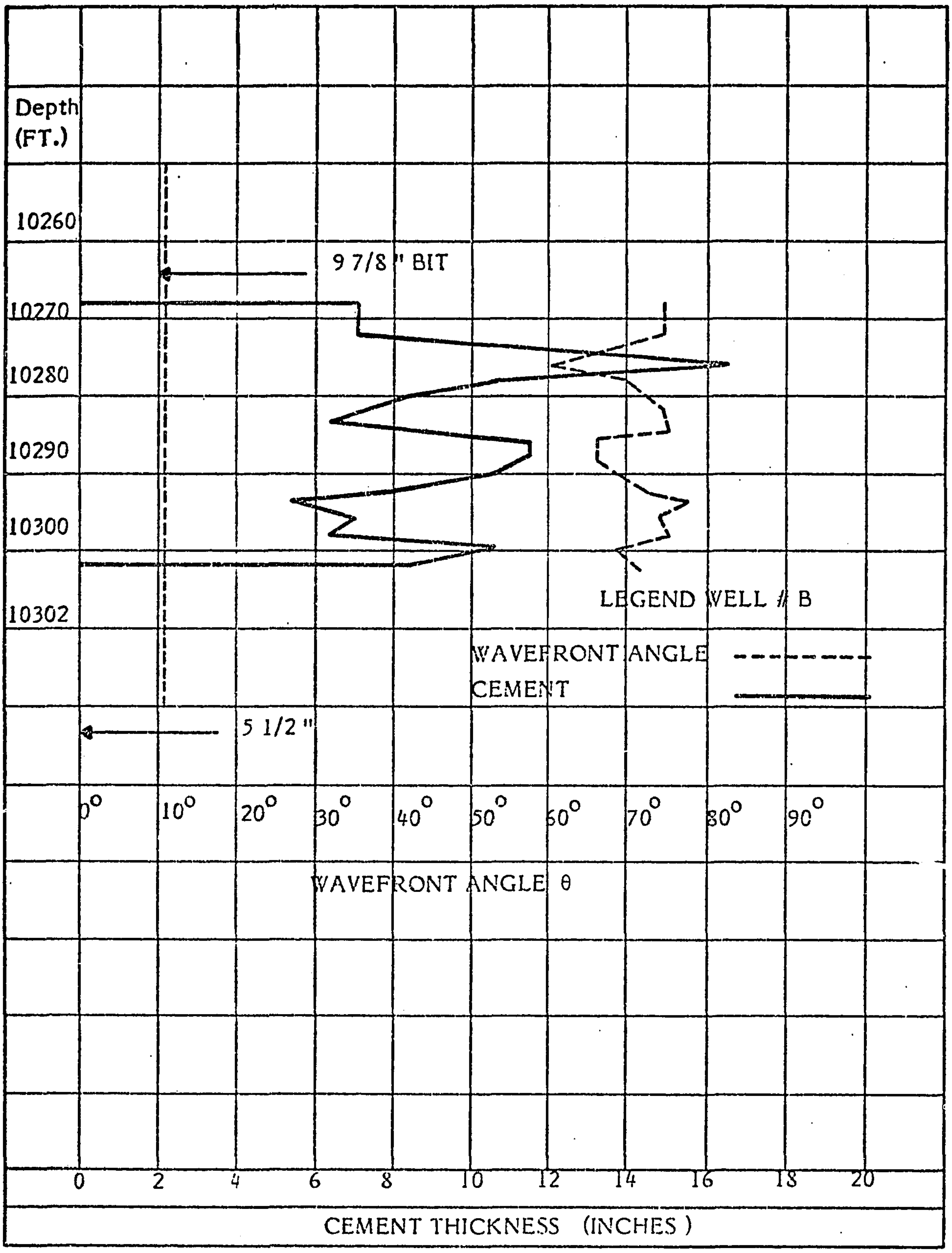

Figure IV-7 Cement Thickness and Wavefront Angle for Well # B 10300' zone

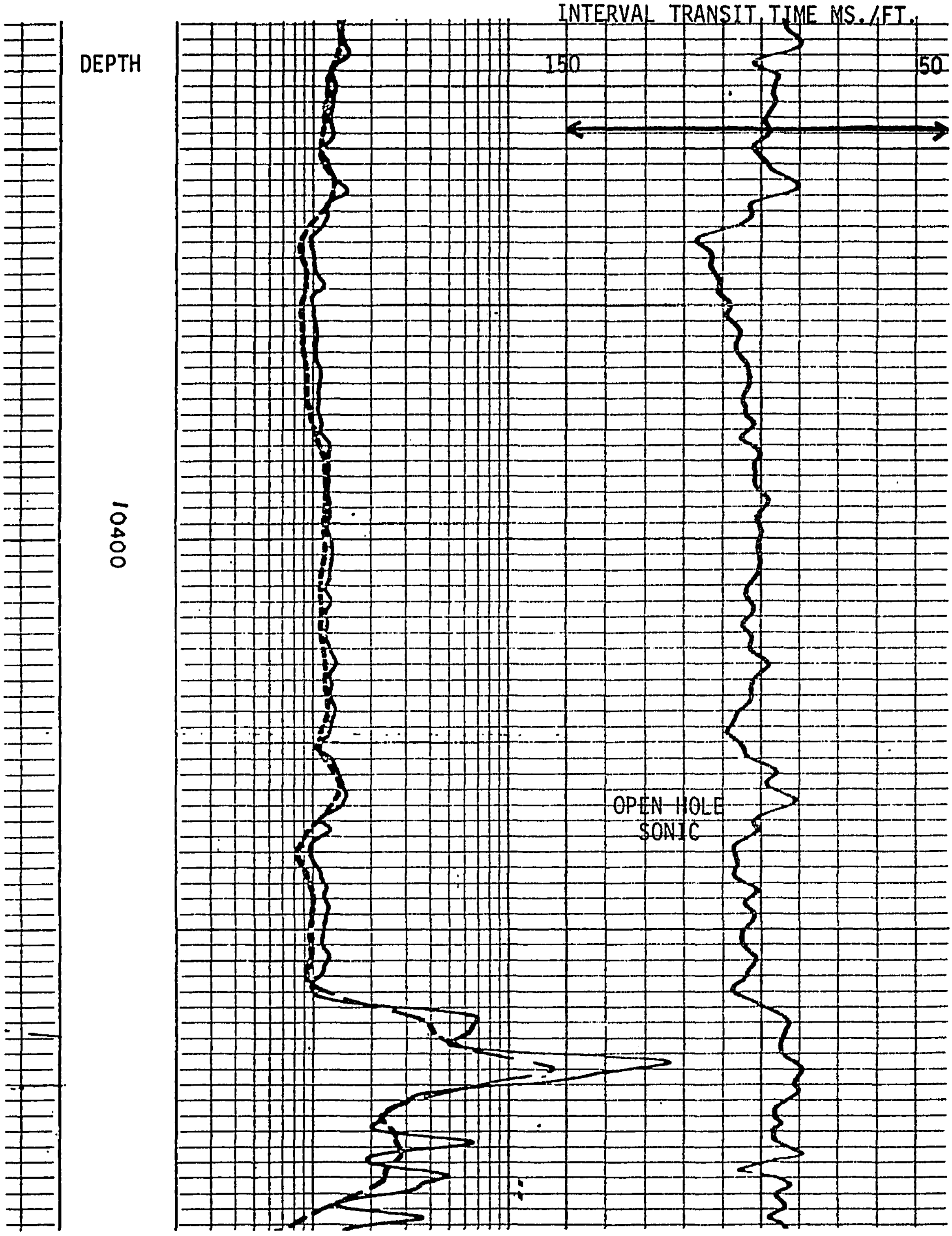

Figure IV-8 Open Hole Sonic Log for Well # B 10400 ' Zone

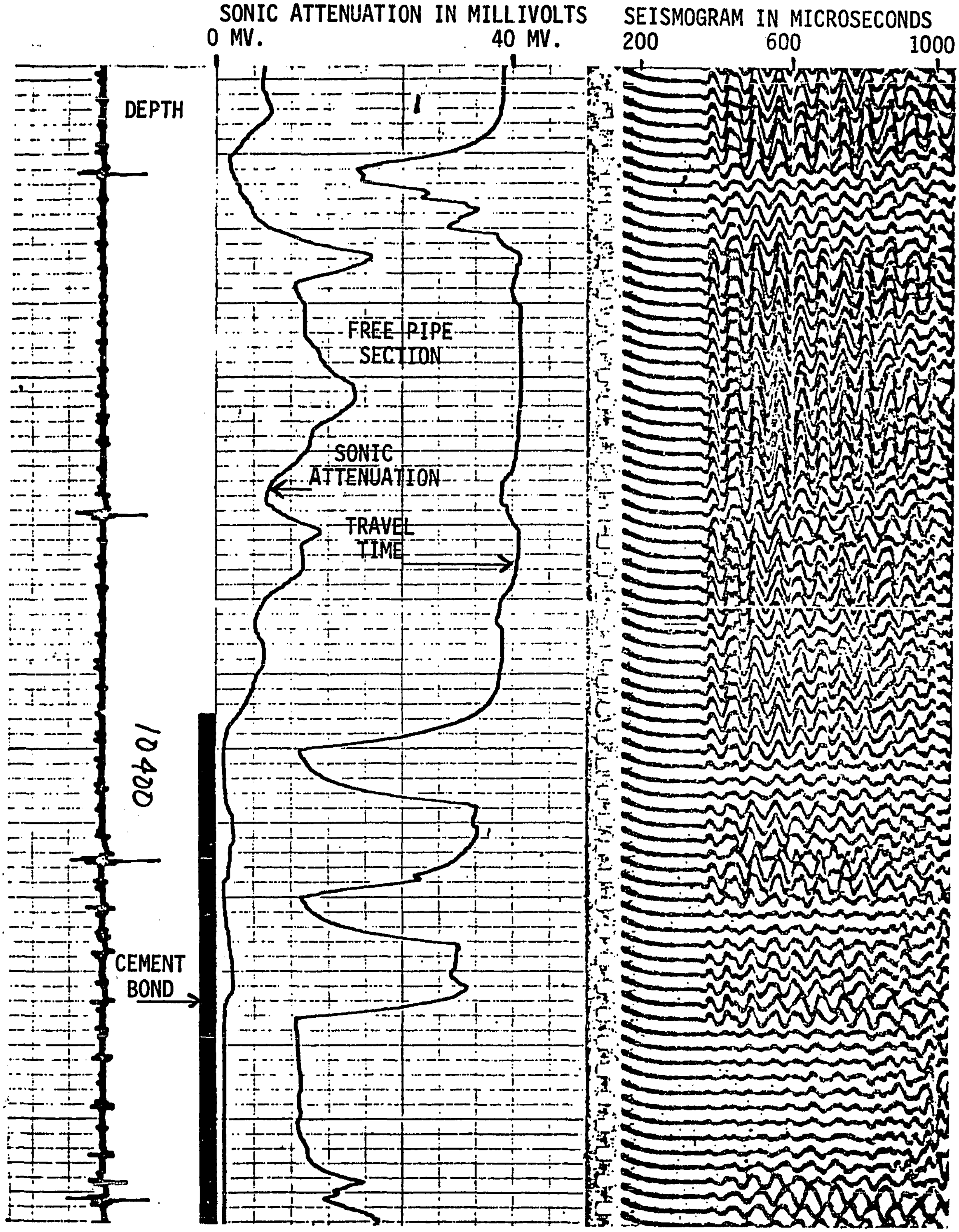

Figure IV-9 Cement Bond Log for Well # B 10400' Zone

TEST RESULTS WELL # B: 10400 Zone

DEPTH FT.	OPEN HOLE SONIC DTf µS./FT.	SEISMOGRAM ST µS.	WAVEFRONT ANGLE θ DEG.	CEMENT THICKNESS IN.
10396	98	440	71.19	9.67
10398	101	435	73.23	8.49
10400	101	450	67.75	11.72
10402	100	430	75.60	7.15
10404	101	430	75.60	7.15
10406	104	437	72.38	8.98
10408	103	437	72.38	8.98
10410	103	430	75.60	7.15
10412	104	430	75.60	7.15
10414	98	435	73.23	8.49
10416	102	430	75.60	7.15
10418	102	430	75.60	7.15
10420	106	420	82.60	3.35
10422	108	450	67.75	11.72
10424	106	435	73.23	8.49
10426	104	430	75.60	7.15
10428	96	430	75.60	7.15
10430	98	430	75.60	7.15
10432	92	425	78.52	5.54
10434	102	425	78.52	5.54
10436	103	475	61.26	15.90
10438	107	475	61.26	15.90
10440	107	480	60.19	16.64

DEPTH FT.	OPEN HOLE SONIC DTf μS./FT.	SEISMOGRAM ST μS.	WAVEFRONT ANGLE θ DEG.	CEMENT THICKNESS IN.
10442	104	485	59.18	17.35
10444	104	485	59.18	17.35
10446	102	480	60.19	16.64
10448	105	480	60.19	16.64
10450	105	475	61.26	15.90
10452	102	435	73.23	8.49
10454	104	430	75.60	7.15
10456	107	428	76.69	6.55
10458	100	430	75.60	7.15
10460	93	430	75.60	7.15

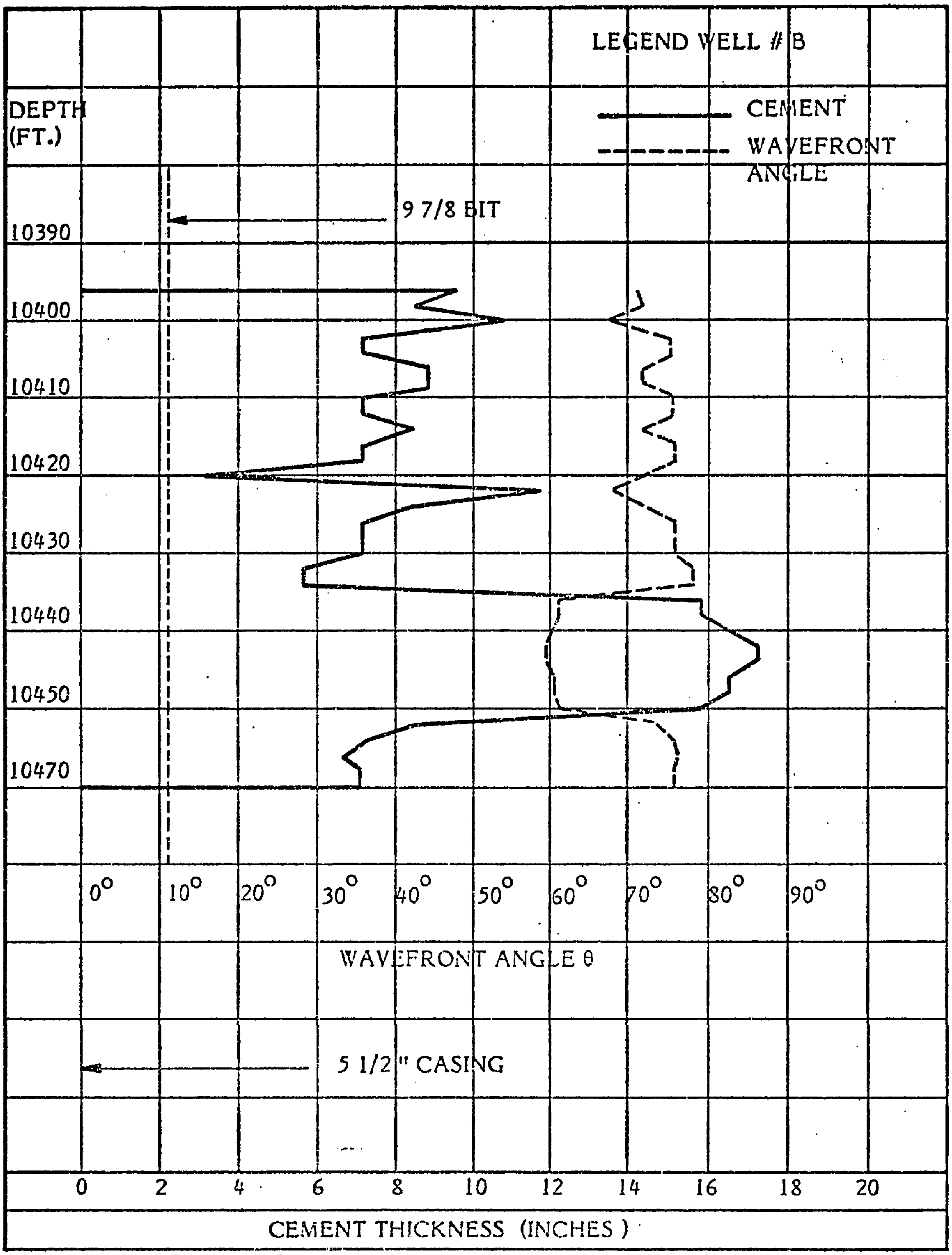

Figure IV-10 Cement Thickness and Wavefront Angle for Well # B
10400 ' Zone

CONCLUSIONS AND RECOMMENDATIONS FOR FURTHER STUDY

The calculated values of the cement thickness compared quite favorably to the effective caliper. These results also justified the Wavefront Angle approximation of the multi-layer system.

The measurement would have been impossible to make if the casing had a thickness greater than 1/4 wavelength as it is considered transparent to that size. Snell's Law does not allow for a refraction angle at the casing / cement boundary to cause a critical angle at the cement / formation interface.

From results taken at Well # B it is obvious that the Wavefront Angle reads inversely with cement thickness in reflection analysis and varies according to the formation in refraction zones. More research would be needed to determine if the Wavefront Angle could be utilized as a correlation tool to identify subsurface geology.

Longer detector spacings and extended seismogram time scales will not cause formation signals to be seen in unconsolidated or soft formations. This has been a factor in South Louisiana operations where formation signals will be seen when their transit times are lower than that of the bonded cement.

For the major part of the South Louisiana sub-surface geology the CBL path of interest is a reflection instead of the well known refraction paths seen in the literature.

Problems:

The present Seismogram time scale used in most cement bond logs is hard to read. In South Louisiana, due to reflection, the cement thickness changes rapidly within 100 microseconds. A better time scale is needed to be able to differentiate between 310 and 315 Microseconds, as an example. Since there is a variation of about 6.9 microseconds/inch this could easily be the major cause for errors in cement sheath determination.

The seismogram wave train is subject to distortion and attenuations due to tool decentralization in deviated holes. and the interpreter must be aware of that situation.

Measurement Uncertainty[27]

One of the most important quantities involved is cured cement transit time, ΔT_c, given to be 83.3 microseconds / foot, or 6.9 microseconds / inch.

A variation of .1 μ Sec / In in ΔT_c would be considered reasonable and requires fair knowledge of the cement. This yields a 0.140 inch uncertainty per inch of cement involved.

If the cement is not known, the value of ΔT_c does change slightly with types of cement and curing time, increasing to nearly 9 microseconds / inch for pozzolan light cement. This would yield a 0.3 inch uncertainty per inch of cement.

The fact that the cement transit time is not exactly known could partially acount for the difference in measurement of cement thickness by the Cement Bond Log as compared to the open hole caliper.

APPENDIX I-A

INFORMATION ON CEMENT THICKNESS W/AMERADA HESS CORPORATION

05/09/77

Discussion with possibility of use for cement thickness evaluation.

1. Determine if vugs exist that cement filled up.
2. Compare open hole caliper with acoustic caliper cement thickness at later date for another zone completion.
3. Determine well head fill-up.
4. Zones of interest for possible squeeze at lesser cement thickness.
5. This service would be a specialized service for determination of thinnest cement for structure of the cased well/perforating consideration.
6. By talking to two engineers at Amerada Hess, this type of specialized service would benefit sales as an extra selling point.

LEE

APPENDIX I-B

INFORMATION ON CEMENT THICKNESS UTILITY W/WESTERN CO. OF N.A. AND UNIVERSITY OF OKLAHOMA:

05/20/77

1. From an Engineering point of view, it provides mathematical proof and an aid to the Bond Log.
2. Bond failures will occur at weakest plane and can so be determined for communication problems.
3. Erroneous tops of cement in Temperature Surveys can be determined due to thick cement conditions.
4. The Fill-Up Efficiency can be determined with more accuracy.

   Eff. = Volume of Cemented Annulus / Volume of Cement Slurry
5. Wash-out zones can be effectively calipered overcoming open hole caliper limitations.
6. Perforating considerations can be taken when there is danger of channeling due to cement fracture.
7. Acid concentrations in Stimulation treatents may be taken into consideration to avoid channeling in thin cement structures.
8. Thin cement structures are also a major consideration when pumping sand into formation fractures.
9. Cement bond to mudcake could also be detected by under Bit-Size thickness measurements in high permeable zones.

10. An acoustical subsurface image of the well structure can be obtained.

GW

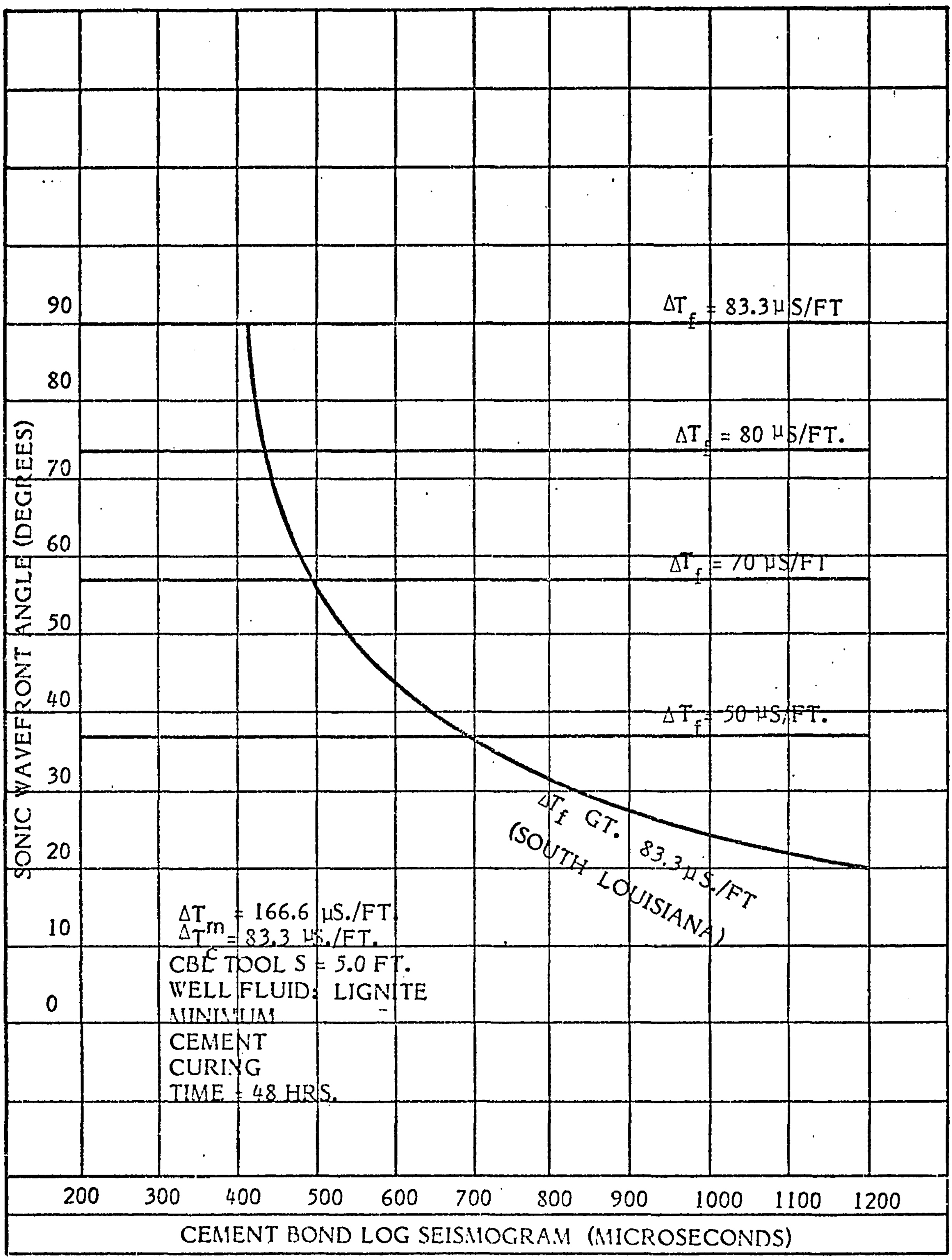

APPENDIX II-A
Seismogram/Wavefront Angle Formation Response

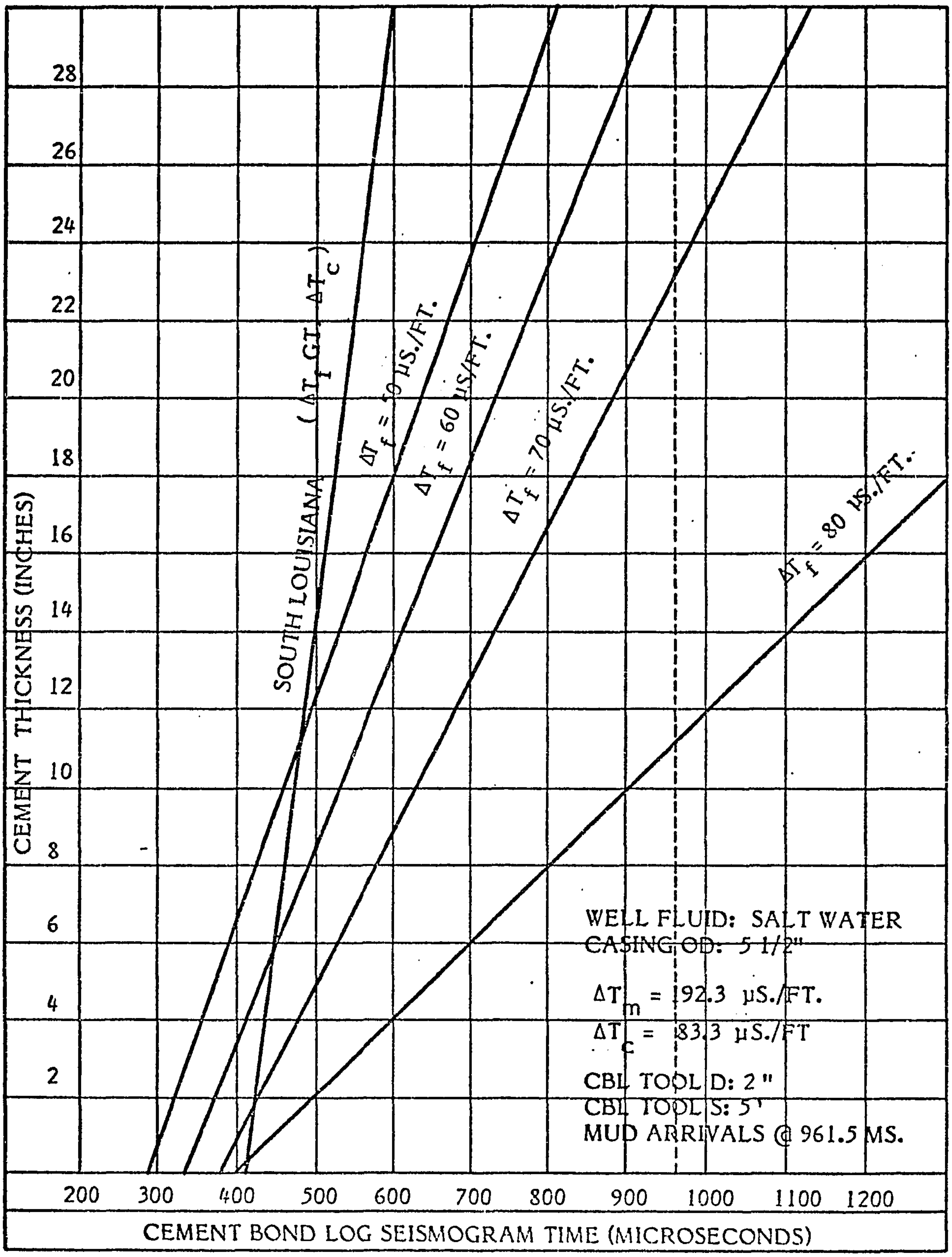

APPENDIX II-B
Seismogram / Cement Thickness Chart for Salt Water

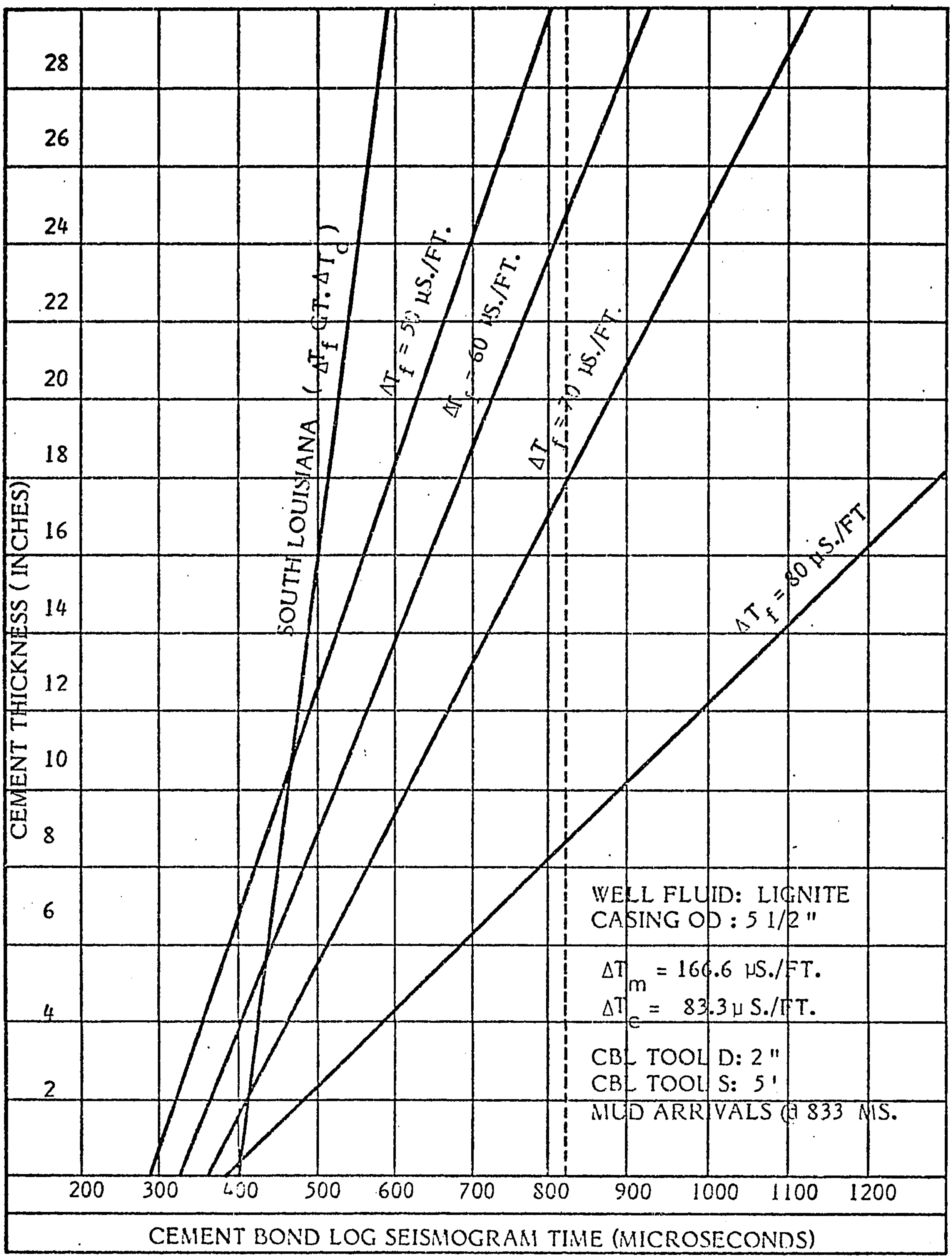

APPENDIX II-C
Seismogram / Cement Thickness Chart for 5 FT. Spacing

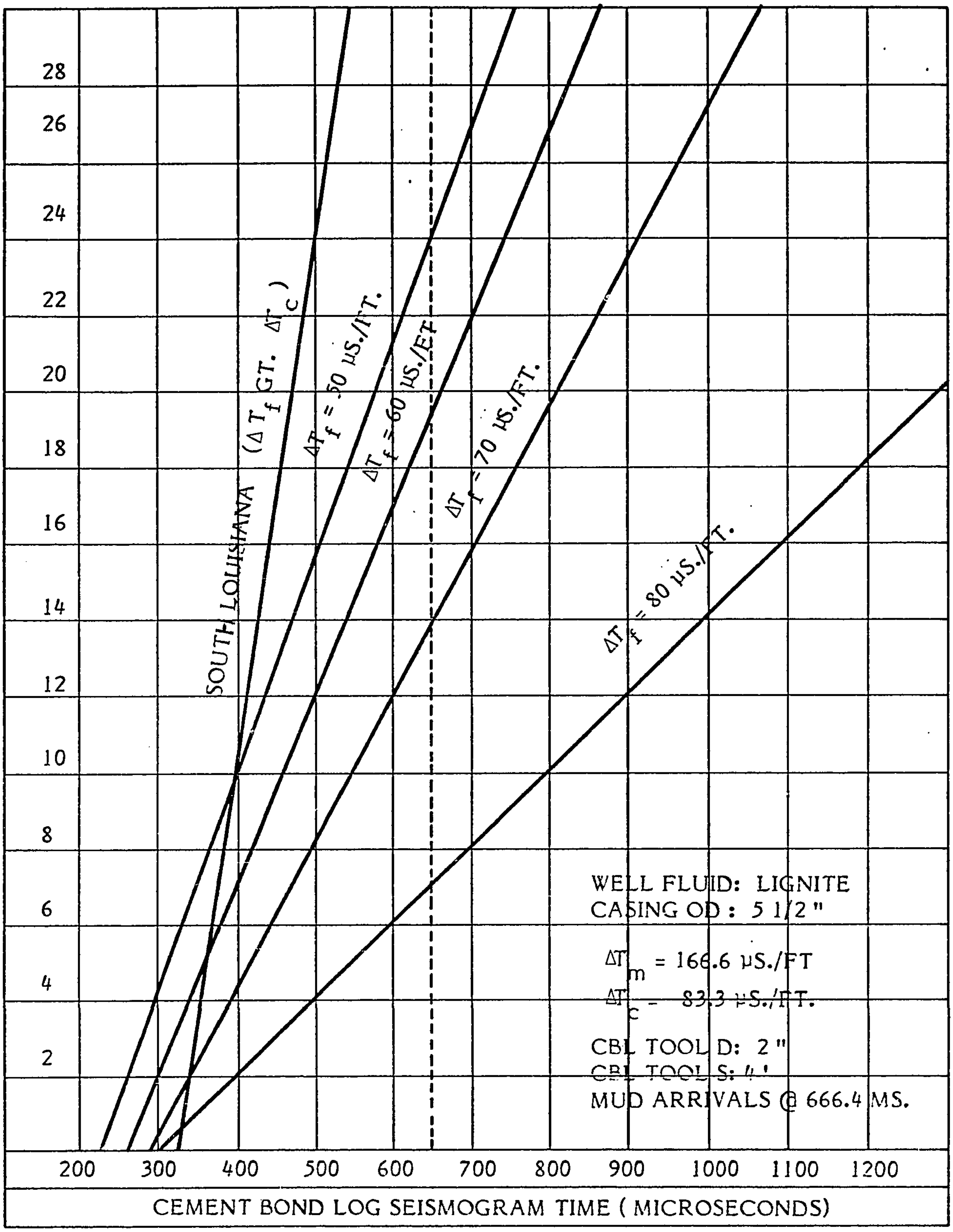

APPENDIX II-D

Seismogram / Cement Thickness Chart for 4 Ft. Spacing

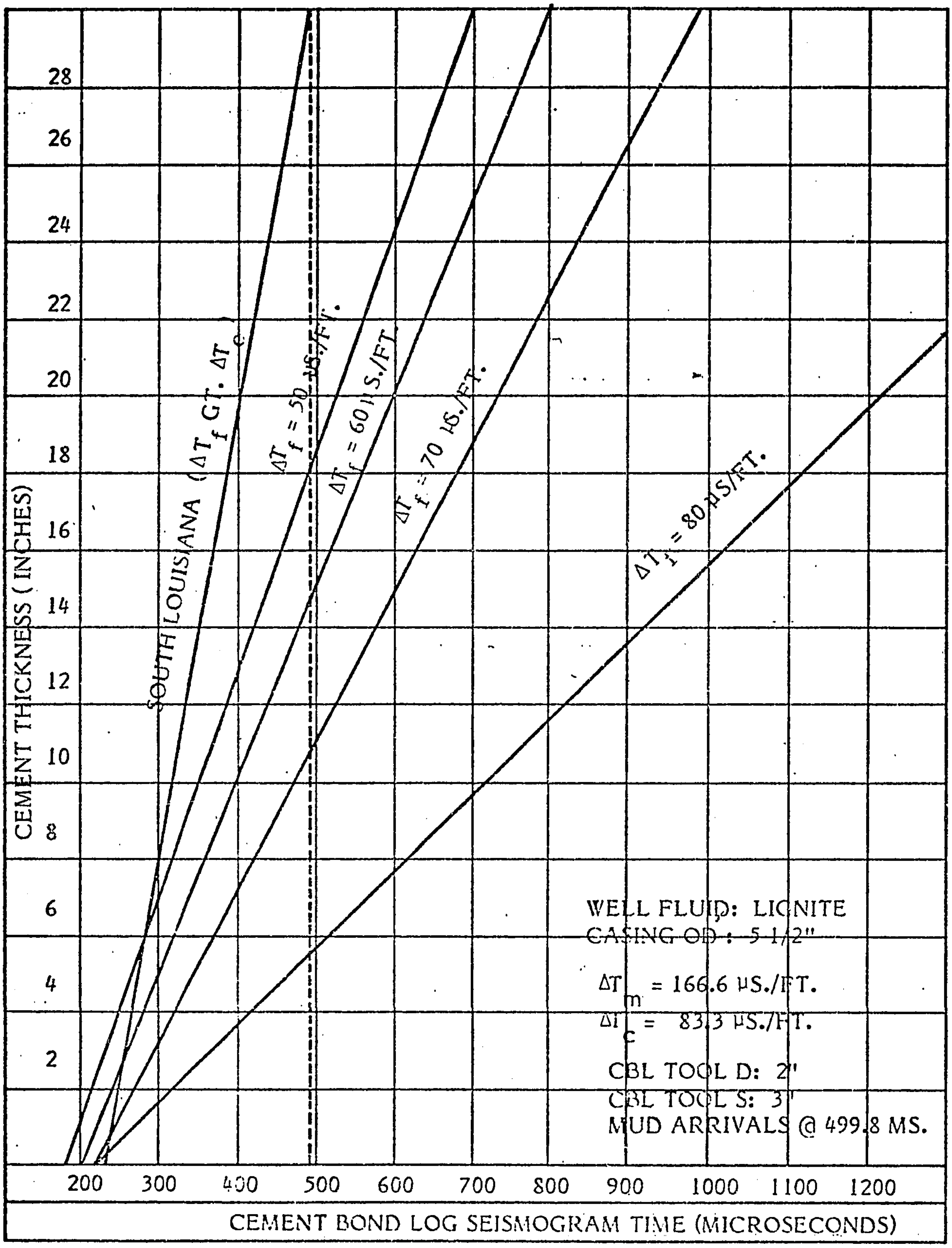

APPENDIX II-E
Seismogram / Cement Thickness Chart for 3 Ft. Spacing

SONIC VELOCITY IN NaCl SOLUTIONS
APPENDIX III - A
Courtesy of Gearhardt-Owen Inc.

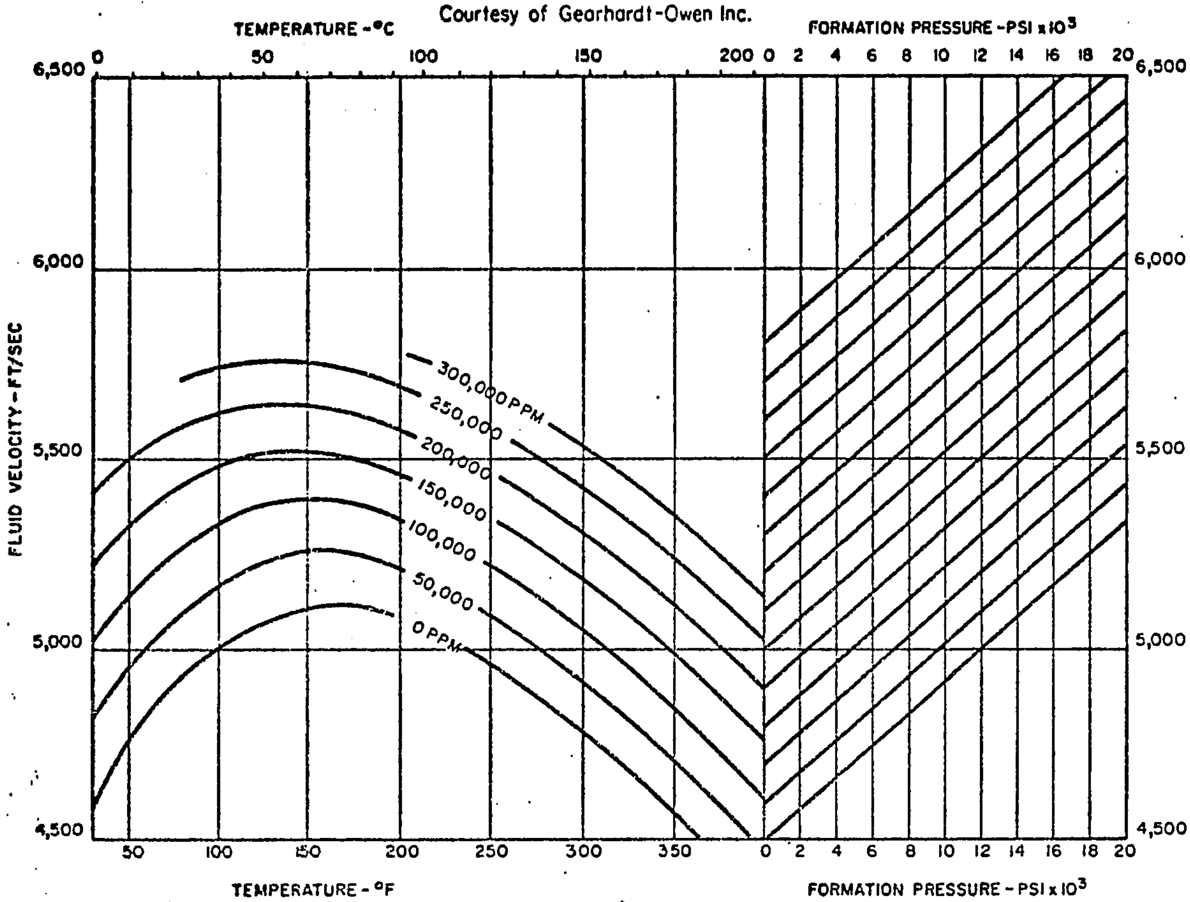

POROSITY FROM SONIC LOG
APPENDIX III - B

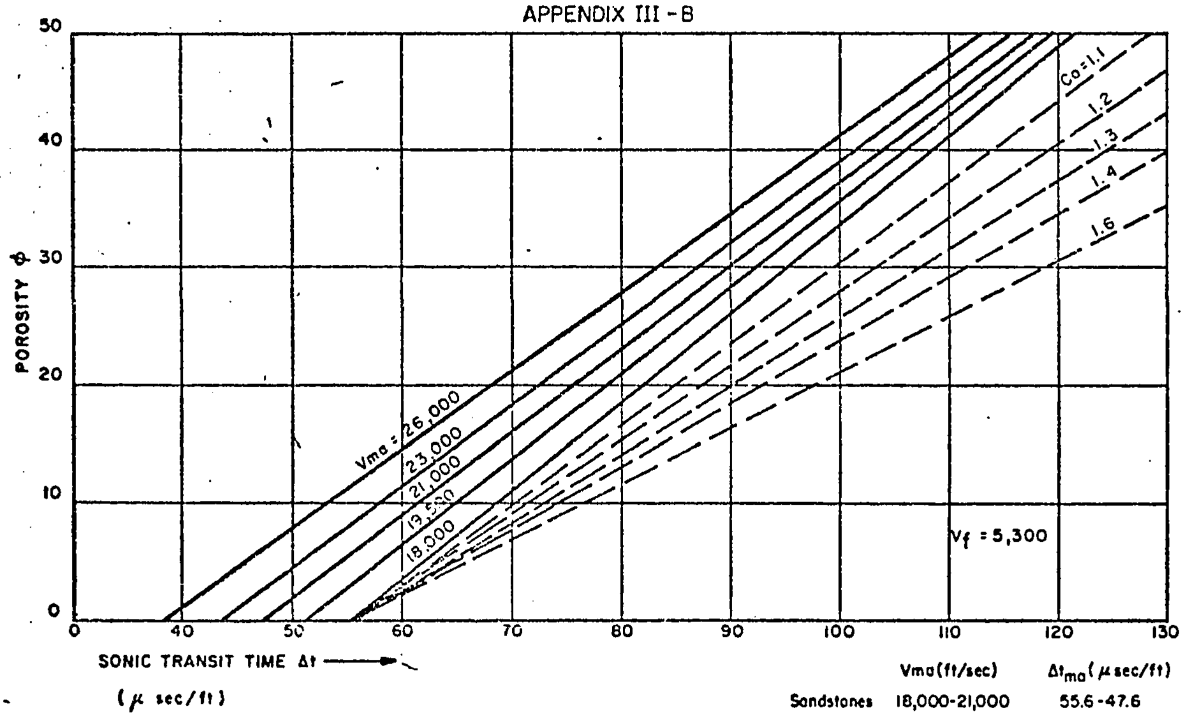

Courtesy of Schlumberger Inc.

	Vma (ft/sec)	Δt_{ma} (μ sec/ft)
Sandstones	18,000-21,000	55.6-47.6
Limestones	21,000-23,000	47.6-43.5
Dolomites	23,000-26,000	43.5-38.5

APPENDIX IV

TEXAS INSTRUMENTS SR-52 PROGRAM CODE

KEY CODE	KEY	KEY CODE	KEY
00	0	46	2nd LBL
01	1	47	2nd CMs
02	2	48	2nd EXC
03	3	49	2nd PROD
04	4	50	2nd st flg
05	5	51	SBR
06	6	52	EE
07	7	53	(
08	8	54	)
09	9	55	÷
10	2nd E'	56	2nd rtn
11	A	57	2nd fix
12	B	58	2nd dsz
13	C	59	2nd π
14	D	60	2nd if flg
15	E	65	X
16	2nd A'	67	2nd 7
17	2nd B'	68	2nd 8
18	2nd C'	69	2nd 9

KEY CODE	KEY	KEY CODE	KEY
19	2nd D'	70	2nd if err
20	2nd 1/x	75	-
22	INV	77	2nd 4
23	lnx	78	2nd 5
24	CE	79	2nd 6
25	CLR	80	2nd if pos
27	2nd INV	81	HLT
28	2nd log	85	+
29	2nd x!	86	2nd rset
30	2nd $\sqrt{x}$	87	2nd 1
32	sin	88	2nd 2
33	cos	89	2nd 3
34	tan	90	2nd if zro
35	$x\sqrt{y}$	91	RUN
36	2nd IND	93	.
37	2nd D.MS	94	+/-
38	2nd D/R	95	=
39	2nd P/R	96	2nd read
40	2nd x^2	97	2nd list
41	GTO	98	2nd prt
42	STO	99	2nd pap
43	RCL		
44	SUM		
45	y^x		

VITA

Giorgio Mario Wiercinski was born in Alezio, Italy on January 29, 1948, to Siegmund and Liliana Wiercinski. He attended the Colegio San Luis High School in Antofagasta, Chile and graduated in December 1965. He completed his Bachelor of Science (1970) and Master of Engineering (1972) in Electrical Engineering from Texas A&M University.

While attending the University of Oklahoma under the Doctor of Engineering program, he was employed by the Western Company of North America as District Electrical Engineer in Lafayette, Louisiana. His permanent mailing address is Villa Musti, Alezio, Italy.

This research was supported by The Western Company of North America's Wire Line Division under Gulf Coast Region operations and monitored by Western's Technical Center in Fort Worth and the University of Oklahoma.

This dissertation was typed by Barbara Mullikin.

REFERENCES

(1) Smith, D. K., Cementing, Halliburton, Duncan, Oklahoma, AIME (1976).

(2) Teplitz, A. J., An Investigation of Oil Well Cementing, Drilling and Production Practices, API (1946).

(3) Folmar, L. W. ; Methods of Detecting T.p of Cement behind Casing API-Oil Well Cementing Practices in the U.S. (1959).

(4) Pardue, G. H., et al, Cement Bond Log - A Study of Cement and Casing Variables: J.P.T. V. XV No. 5 (1963).

(5) Grosmangin, M., et al, A Sonic Method for Analyzing the Quality of Cementation of Borehole Casing, J.P.T., V, XIII, No. 2.

(6) Pickett, G. R., Prediction of Interzone Fluid Communication behind Casing by Use of the Cement Bond Log: S.P.W.L.A. Transactions.

(7) Suman, G. O., Cementing Oil & Gas Wells, World Oil, Nov. (1977).

(8) Zemanek, J., The Borehole Televiewer: 43rd Ann. Fall Meet S.P.E. of A.I.M.E. (1968).

(9) Chisholm, J.P. & Patterson, G. D., Sonar Caliper/LPG Storage Surveys: PE, V. XXX, Sec. B, No. 1 (1958).

(10) Urick, R. J., Lectures on Marine Acoustics TAMU, Volume II, Naval Ordnance Laboratory, U.S. Navy (1971), 73.

(11) Caruthers, J.W., Lectures on Marine Acoustics, Volume I, Sea Grant TAMU-SG-71-403 (1971).

(12) Guyod, Hubert and Shane, L.E., Geophysical Well Logging, Volume I (1969), 137, 183.

(13) Fahlquist, D. A., Lectures on Marine Acoustics TAMU, Volume II, Texas A&M University (1971), 117.

(14) Novarini, J.C., Lectures on Marine Acoustics TAMU, Volume II (1971), Hydrographic Office, Argentine Navy (1971), 13.

(15) Officer, C.B., Introduction to the Theory of Sound Transmission in the Ocean, McGraw-Hill, New York (1958).

(16) Officer, C. B., Introduction to the Theory of Sound Transmission, McGraw-Hill, New York (1958).

(17) Wyllie, M.R.J., The Fundamentals of Well Log Interpretation, Academic Press (1963), 165.

(18) Western Wire Line Services Bulletins, The Western Co. of North America, Fort Worth (1976), 10.1, 10.2.

(19) Veach, Charles, Private Communication, The Western Company of North America, Technical Center, Fort Worth, Texas (1976).

(20) Caruthers, J.W., Lectures on Marine Acoustics, Volume II, Sea Grant TAMU-SG-71-404 (1971).

(21) Engineers Handbook, The Western Company of North America, Fort Worth (1977), 5-1, 7-0.

(22) Kingler, L.K. and Frey, A.R., Fundamentals of Acoustics, John Wiley (1962).

(23) Sadras, W., Evaluacion de las Formaciones en la Argentina, Schlumberger Inc. (1973), 178.

(24) Slotnick, M.M., Lessons in Seismic Computing, Society of Exploration Geophysics (1959).

(25) Suman, G.O., Jr., Cementing Oil and Gas Wells, World Oil, April (1977).

(26) Texas Instruments, Inc., Programmable Slide-Rule Calculator SR-52 Work Book, Dallas (1977).

(27) Tucker, D.G., and Glazey, B.K., Applied Underwater Acoustics, Pergamon Press, London (1966).

(28) Urick, R.J., Principles of Underwater Sound for Engineers, McGraw-Hill, New York (1967).